PERSPECTIVE

Dalton
www.rsc.org/dalton

Supported molecular catalysts: metal complexes and clusters on oxides and zeolites

Javier Guzman and Bruce C. Gates*
Department of Chemical Engineering and Materials Science, University of California, Davis, California, 95616, USA. E-mail: bcgates@ucdavis.edu

Received 24th March 2003, Accepted 17th May 2003
First published as an Advance Article on the web 16th June 2003

When metal complexes and clusters are bonded to oxide or zeolite supports, they may combine the technological advantages of solid catalysts (robustness for high-temperature operation, lack of corrosiveness, ease of separation from products) with the selectivity of soluble molecular catalysts. Supported mononuclear metal complexes are typically synthesized by the reaction of a mononuclear organometallic compound with oxygen atoms or OH groups of the support, giving structures shown by infrared, X-ray absorption, and NMR spectroscopies and density functional theory to be analogous to those of molecular species, but with the support playing the role of a multidentate ligand, bonding strongly to the metal and holding the groups apart from each other on the support surface. Some supported metal complexes have new and unexpected catalytic activities. Supported metal clusters are formed by adsorption or surface-mediated synthesis of metal carbonyl clusters, which under some conditions may be decarbonylated on the support with the metal frame remaining essentially intact. The decarbonylated clusters are bonded to the supports by metal–oxygen bonds similar to those characterizing supported metal complexes; even noble metals in clusters on supports at the metal–support interface are cationic, and the metal–oxygen distances are about 2.1–2.2 Å, matching the distances in mononuclear metal complexes with metal–oxygen bonds. Metal clusters are preferentially bonded at defect sites on oxide surfaces. The catalytic activities of supported metal clusters of only a few atoms are distinct from those of bulk metals; the supports act as ligands affecting the catalysis.

1. Introduction

Molecular catalysts in solution offer the advantages of accessibility to reactants and uniqueness of structure that confer high activity and selectivity. In contrast, solids offer catalytic sites only at their surfaces, which are non-uniform, often having a spectrum of reactivities and low catalytic selectivities, offsetting the advantages of ease of separation from products, lack of corrosiveness, and robustness for operation at high temperatures. The prospect of combining the advantages of the two classes of catalysts has motivated synthesis of solids with surface catalytic groups that are molecular analogues. Some such catalysts might be considered primitive mimics of enzymes, which consist of biologically optimized catalytic sites in organic matrices.

The field of nearly molecular supported catalysts is not new, dating back at least to pre-World War II applications of sulfonic acid ion-exchange resins as replacements for soluble strong-acid catalysts.[1] With the recent emphasis on environmental protection, the need for solid catalysts to replace liquids has grown, and the field is burgeoning, extending from labor-

Javier Guzman was born in 1977 in Mexico City, Mexico. He graduated with honors from Universidad Autonoma Metropolitana, Mexico City, in 1999, with a B.S. degree in chemical engineering. He joined Prof. Bruce Gates' catalysis research group at the University of California, Davis, in the fall of 1999 with the sponsorship of the Fulbright Commission and Conacyt. He has developed new methods for synthesizing supported gold clusters and investigated a family of supported molecular catalysts including gold complexes on metal oxides, which were characterized with spectroscopic techniques during catalysis. He will soon earn his Ph.D. degree in chemical engineering.

Bruce C. Gates is Professor of Chemical Engineering at the University of California at Davis, where his research group investigates supported metal complexes and metal clusters, working on their synthesis, spectroscopic and microscopic characterization, and testing as catalysts; the group specializes in characterization of catalysts in the functioning state by methods including X-ray absorption spectroscopy and infrared spectroscopy. Gates is the author of the textbook Catalytic Chemistry *(Wiley, 1992) and a co-author of* Chemistry of Catalytic Processes *(McGraw-Hill, 1979). He edits the series* Advances in Catalysis *and co-edited* Metal Clusters in Catalysis *and* Surface Organometallic Chemistry: Molecular Approaches to Surface Catalysis.

Javier Guzman

Bruce C. Gates

DOI: 10.1039/b303285j

atory preparative chemistry to industrial applications. Many catalysts used in the laboratory, exemplified by those supported on functionalized organic polymers or on organic groups bonded to porous inorganic solids, are close analogues of soluble catalysts, with the catalytic groups present in surroundings resembling organic solvents. Such supported catalysts (and reagents) are used widely, even in syntheses involving numerous steps,[2] but they typically suffer from a lack of stability, especially at high temperatures.

A high degree of catalyst stability has evidently been achieved, however, in the commercial Acetica™ process for methanol carbonylation to give acetic acid;[3] a vinyl pyridine resin is used to support the anionic rhodium complex catalyst. Prospects for large-scale applications of polymer-supported catalysts extend to numerous reactions occurring under mild conditions, including asymmetric syntheses.[4]

Our focus is on more robust catalysts, supported on inorganic solids (metal oxides and zeolites). In some respects, nearly molecular catalysts on such supports serve as models of the structurally complicated catalysts used in petroleum refining and large-scale chemical production.[5–7]

Most successful catalysts, ranging from small molecules and ions to enzymes and surfaces, present coordinatively unsaturated metal centers for bonding of reactants as ligands that are converted under the influence of the metal center and neighboring ligands. Thus, many attempts to prepare supported catalysts have begun with metal-containing compounds that react with a surface to give complexes anchored through support ligands. When the goal is precise synthesis to give a uniform, selective supported catalyst, obvious precursors are metal complexes with reactive ligands that can be replaced by the support. Metal complex precursors, especially organometallics, are preferred over metal salts that leave anions such as chloride or nitrate on the catalyst. The goal of precise synthesis of supported mononuclear and polynuclear metal complexes, advocated in early work by Yermakov[8] and Ballard,[9] was important in stimulating what has become a lively, growing field,[10] motivated by prospects of new industrial catalysts. The commercial success of supported ("single-site") metallocenes for alkene polymerization testifies to the attainability of the goal.[11]

The following account is focused on the chemistry of oxide- and zeolite-supported metal complexes, including metal clusters. Examples are taken from the literature broadly, with threads of continuity taken from the authors' work. The chemistry involves

(a) synthesis on surfaces,

(b) structure determination by spectroscopic methods, sometimes combined with microscopy and other methods for determining composition and structure, and

(c) reactivity and catalysis.

The available results demonstrate the following:

(a) surface chemistry that closely resembles that of molecular analogues in solution,

(b) fundamental understanding of catalysis at a depth that is unusual for solid catalysts,

(c) examples of catalysts with unforeseen activities and prospects for application, and

(d) insights into the properties of supported industrial catalysts, which are typically highly non-uniform in structure.

Transition metal complexes in solution are used as catalysts in many industrial processes.[12] Early work with analogous supported metal complexes[13] led to organic polymer- and oxide-supported catalysts for alkene hydrogenation, alkene hydroformylation, and methanol carbonylation, among many others.[3,10,13] These catalysts failed to find industrial application, primarily because of leaching of the metal into solution and lack of stability of the catalysts, including the ligands bonded to the support (*e.g.*, phosphines); sometimes the metal was reduced to the zero-valent state, forming clusters or particles on the support.

The problem of leaching of metals is likely to be persistent and limit applications of such catalysts in the presence of liquids; to minimize leaching into solution, the catalytically active complex must remain tightly bonded to the support at each step of the catalytic cycle.

In contrast, when a supported metal complex is used with gas-phase reactants, leaching is avoided, and—if the metal–support combination is stable—the catalyst can be used at high temperatures. Thus, robust metal oxides are appealing supports, and the most useful are porous solids that offer high internal surface areas for high loadings of catalytic groups.

Industrially important examples of oxide-supported mononuclear metal complex catalysts include the metallocenes used for alkene polymerization.[14] Catalyst deactivation is not a dominant issue in the polymerization processes because yields of polymer are high and the catalyst, enveloped by the growing polymer chains, remains in the product as a minor impurity. The Phillips catalyst, the first of these applied commercially, is a chromium complex on silica.[15] Newer polymerization catalysts also include supported metal (*e.g.*, Zr) complexes, which are used in the presence of a structurally complex co-catalyst, methylalumoxane (MAO).[16] Other oxide-supported catalysts are complexes of tungsten and of rhenium, used for alkene metathesis. A supported zirconium complex catalyst for depolymerization of polyalkenes by hydrogenolysis was reported recently,[17] and a silica-supported tantalum hydride complex has been found to be catalytically active, even at room temperature, for a new reaction, alkane disproportionation.[18] Some details are given below.

Notwithstanding the novelty and practical importance of supported metal complex catalysts, they are much less well understood than transition metal complexes in solution. But, as described here, understanding of their structure, bonding, and catalytic performance is emerging rapidly as physical methods are brought to bear on the characterization of samples synthesized to be structurally well-defined.

2. Chemistry of supported mononuclear metal complexes

Researchers investigating metal complexes on supports face limitations that do not pertain to such compounds in solution or in the crystalline state. A chemist preparing a supported metal complex does not have the luxury of column chromatography, crystallization, or related purification methods for removal of undesired products, because they typically remain on the support along with the desired species. The supported species are often distributed non-uniformly on the internal surface of the support, and support surfaces are themselves intrinsically non-uniform at the atomic, nano, and even micro scales. Consequently, structure determination by X-ray diffraction (XRD) crystallography is generally not feasible. Furthermore, spectroscopic methods require cells serving as reactors for sample treatment and equipment that is lacking in many laboratories. Consequently, the degree of uniformity of supported metal complexes is difficult to assess and has no doubt been overestimated in some reports.

In the following sections, we summarize methods and results characterizing the composition, structure, bonding, reactivity, and catalytic properties of oxide- and zeolite-supported metal complexes, choosing examples that we believe to be relatively well defined.

2.1 Synthesis

Supported metal complex catalysts are typically prepared by the reaction of a metal complex incorporating reactive ligands (such as alkyls, allyls, or carbonyls) with oxygen atoms or OH groups of oxide or zeolite supports. The metals in the resultant supported complexes are typically bonded to the support

oxygen atoms. In some preparations, oxidative addition of an O–H ligand of an oxide support surface to a metal center of an organometallic complex leads to anchoring of the metal complex. These and other synthetic surface reactions are reviewed elsewhere.[19,20]

2.2. Composition

Determination of the compositions of supported metal complexes typically involves elemental analysis of the solid to determine the metal content (and possibly components of the ligands), for example, by X-ray fluorescence or inductively coupled plasma analysis. Often the synthesis involves a reaction that anchors all of the metal in a soluble precursor to the support, followed by complete removal of the solvent by evacuation, so that the metal content of the catalyst is determined by how much metal is added in the synthesis.

The resultant supported metal species often incorporate reactive ligands retained from the precursor, such as alkyls or carbonyls. Quantitative methods for determination of the gaseous products formed in the synthesis and/or in subsequent conversion of the ligands in the surface-bound complex include collection of all the gas-phase products and their analysis by techniques such as gas chromatography. The compositions of the ligands are inferred from the gas-phase analysis, sometimes combined with spectra of the surface species.

For example, it has been shown[21] that $Rh(\eta^2\text{-}C_3H_5)_3$ reacts at room temperature with hydroxyl groups on the surfaces of silica, titania, and alumina, forming a supported bis(allyl)-rhodium complex and a molecule of propene. Subsequent exposure of these grafted complexes on silica to H_2 led to the formation of metallic rhodium clusters or particles,[22] and most of the allyl groups were removed as propane and hexanes, as determined qualitatively by gas-phase analysis by mass spectrometry and quantitatively by gas chromatography.[21] The amount of propane evolved corresponded to approximately one of the two allyl groups of the supported bis(allyl)rhodium complex. The measured quantity of *n*-hexane + 2-methylpentane (0.7 C_3 groups/Rh) was slightly less than that expected (1.0 C_3 groups/Rh) for the formation of metallic rhodium and regeneration of surface hydroxyl groups.[21,23] A small amount of CO coordinated to the resultant metallic rhodium was observed, with the oxygen of the CO arising from the water or hydroxyl groups of the support, as indicated by experiments with samples that had been treated with $^{18}O_2$, D_2O, or $H_2{}^{18}O$.[23]

In an alternative method of analysis, one can use temperature-programmed decomposition (or reduction or oxidation), whereby the solid sample containing the supported metal complex is transferred to a flow system and treated with a gas such as He (or H_2 or O_2), respectively, as the temperature is ramped at a specified rate, with the product gas being analyzed periodically by a mass spectrometer to determine its composition and continuously by a calibrated thermal conductivity detector to determine the amount evolved.[24] The temperature-programmed decomposition and reaction methods are rapid and convenient, offering the advantage of information about the spectrum of reactivities of the surface species (indicated by the temperatures at which particular products are evolved and by the identities of these products), which gives evidence pertaining to the degree of uniformity of the surface species as well as the ligand composition. A disadvantage of the temperature-programmed methods is that the required equipment is too specialized to be available in many laboratories.

The characterization of supported metal complexes by temperature-programmed methods is exemplified by results representing MgO-supported rhenium carbonyls[25] (formulated as $[Re(CO)_3\{OMg\}\{HOMg\}_2]$, where the braces denote groups terminating the support) prepared by reaction of $HRe(CO)_5$ or $H_3Re_3(CO)_{12}$ with MgO that had been partially dehydroxylated by treatment in O_2 at 973 K. The reaction converting the surface species initially formed upon adsorption of $H_3Re_3(CO)_{12}$ might be expected to be accompanied by the evolution of CO and/or CO_2 and H_2. Temperature-programmed desorption and temperature-programmed reduction were used to determine the stoichiometry of the reaction. The quantitative results demonstrated the evolution of 2.0 ± 0.2 molecules of CO, 1.0 ± 0.1 molecule of CO_2, and 1.0 ± 0.2 molecule of H_2 per trirhenium cluster. As IR spectra indicated the formation of $[H_2Re_3(CO)_{12}]^-$ as the initially adsorbed species, the following approximate stoichiometry was suggested:

$$\{OMg\}[H_2Re_3(CO)_{12}]^- + \{OMg\} + 2\{HOMg\} \longrightarrow 3[Re(CO)_3\{OMg\}\{HOMg\}_2] + 2CO + CO_2 + H_2 \quad (1)$$

In using these methods of gas-phase analysis as a basis for determination of compositions of surface species, it is important to be aware of errors in the data.

2.3. Structure and bonding

Most evidence of structures of supported metal complexes is spectroscopic, typically IR. Increasingly, extended X-ray absorption fine structure (EXAFS)[26] spectroscopy and ^{13}C and ^1H NMR spectroscopy are being used, among other methods. Interpretation of spectra relies on comparisons with spectra of known compounds, and the best standards are close analogues of the surface species. Because surface species are typically non-uniform, peaks in the IR spectra are usually broader (sometimes much broader) than those of the pure-compound analogues, and the peaks may be shifted as well because the ligands provided by the surfaces may not be closely similar to those in the reference compounds. The broadness of the peaks makes it difficult to distinguish individual surface species from mixtures; mixtures are almost always present because of the non-uniformity of the support surfaces, and the common representations of the surface species usually gloss over the differences in structure of the potential surface sites, depicting instead only the surface atoms in the complex; it is difficult to do better than this.

To improve the bases for determination of surface structures, there is a need for more data characterizing compounds that incorporate ligands that are close analogues of metal oxide and zeolite surfaces. Some of the best appear to be metal oxide clusters such as silsesquioxanes,[27] which are good molecular models of silica because they contain functional groups that represent those present on silica, such as silanols (Si–OH) and siloxane bridges (Si–O–Si) (Scheme 1), but with the advantage that such molecular analogues can be characterized in solution—and in the solid-state, by XRD crystallography. Products of reactions of organometallic complexes with silsesquioxanes can be used as references for comparison with the surface species formed by anchoring the complexes to silica surfaces. Each type of surface silanol group, classified as isolated, vicinal, and geminal, can be represented by a specific corresponding molecular analogue (Scheme 1). Furthermore, there are several molecular analogues for each type of silanol group, and they can be used to model the different local environments of silica and silica-supported metal complexes.

An example of a metal complex bonded to a silsesquioxane is formed by the reaction of an octameric silsesquioxane (Si_8O_{12})-$(p\text{-}C_6H_4CH_2PPh_2)_8$ with $[Rh(CO)_2Cl]_2$ in benzene solution; the product is a yellow powder, $(Si_8O_{12})(p\text{-}C_6H_4CH_2PPh_2)_8(Rh(CO)Cl)_4$, which, after removal of the solvent, is characterized by an IR spectrum with a single ν_{CO} band at 1969 cm^{-1}, which is similar to that observed for a variety of *trans*-$(RPPh_2)_2$-Rh(CO)Cl complexes (≈1970 cm^{-1}).[28] An example of a metallasilsesquioxane is the Pt^{2+}(COD) complex shown in Scheme 2.[29]

More than one spectroscopic technique is almost always needed for a convincing structure determination of a supported

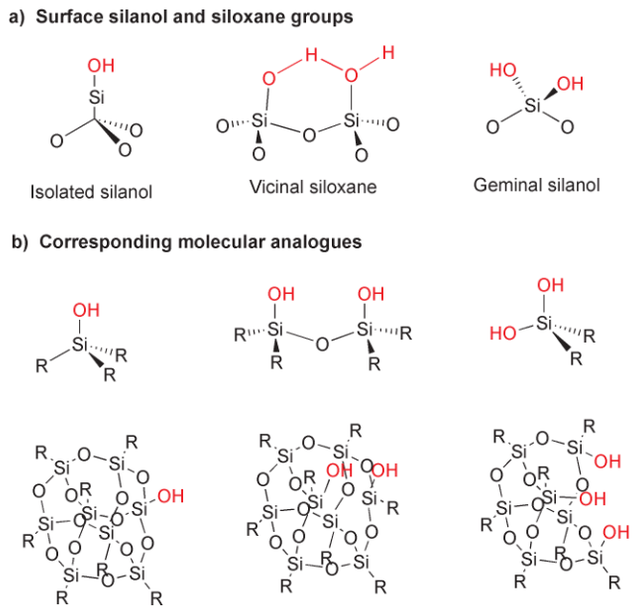

Scheme 1 Representation of surface silanol and siloxane groups in (a) SiO_2 and in (b) the corresponding molecular analogues, polyhedral oligosilsesquioxanes. R represents ligands, such as cyclopentyl, *t*Bu, Ph, *etc*.[27,53]

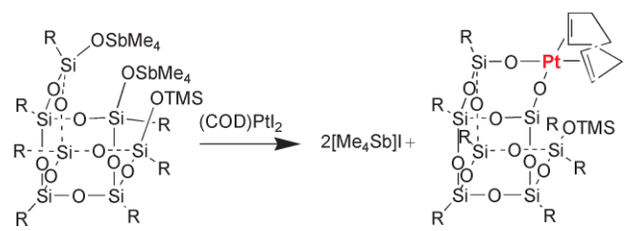

Scheme 2 Reaction of a silsesquioxane with PtI_2(COD) to form an anchored platinum complex.[29]

metal complex (and several techniques may often be insufficient). The lack of applicability of XRD implies that the standard of structure determination of supported metal complexes is well below that of pure-compound analogues. Structures postulated on the basis of only a single spectroscopic technique are common and viewed with skepticism; the possibility of mixtures of surface species and the limitations of analogies to reference compounds often hinder the determination of surface structures.

The presence of mixtures often results from the limitations of synthesis and purification of surface species as well as from the non-uniformity of support surfaces. For example, the surface of silica gel (which is flexible and "soft") typically incorporates Si, Si–OH, Si–O–Si, and Si–$(OH)_2$ groups (Scheme 1) (and perhaps water) in various surroundings, depending on the degree of hydration or hydroxylation. The commonly used support γ-Al_2O_3 incorporates Al–OH groups and Al^{3+} sites (Lewis acid sites), and possibly water, in various surroundings, which are not fully understood; MgO incorporates Mg^{2+} and Mg–OH groups, and possibly water, in various surroundings. The vagueness of the term "various surroundings" may cover lots of uncertainty; the surfaces incorporate groups of various structures and compositions, including defect sites (often of more than one kind) and impurities. Some oxides, exemplified by high-area porous MgO, in contrast to the amorphous silica gel, are characterized by substantial crystallinity, with the solid consisting of microparticles of various sizes and shapes and pores between them and surfaces exposing various crystal planes and edges, with defects such as steps, kinks, and vacancies. Transition aluminas such as γ-Al_2O_3, although often referred to as amorphous because the crystallites are so small, also contain crystallites that expose various faces.

Because of the structural complexity of oxide surfaces and the species formed on them, researchers have been motivated to use supports that are chemically similar to oxides but structurally simpler and more uniform. Such materials are exemplified by zeolites, which are the most common crystalline materials used as catalyst supports (because they are stable, high-area porous solids that are often relatively inexpensive).

Some of the most thoroughly characterized supported metal complexes are zeolite-supported metal carbonyls. These have been prepared, for example, by adsorption of $Rh(CO)_2$(acac) on zeolites (*e.g.*, the faujasite zeolite NaY[30] or dealuminated zeolite Y[31]) or from aqueous solutions of $[Rh(NH_3)_5Cl][OH]_2$ brought in contact with zeolites followed by CO treatment of the resultant material.[32]

The uniformity of the supported species formed by either method is evidenced by the sharpness of their IR bands, illustrated by the results of Miessner and co-workers[32] characterizing species bonded to dealuminated zeolites (*i.e.*, those with low concentrations of Al ions in the aluminosilicate framework)—these provide a low density of sites for binding of cationic complexes and seemingly ensure that such supported complexes are for the most part widely separated from each other—thus, these are nearly "ideal" samples in the sense that the supported groups are site-isolated and, in prospect, nearly uniform. The spectrum of rhodium dicarbonyl on dealuminated Y zeolite (Fig. 1) is characterized by sharp bands; this is contrasted with the spectrum of rhodium dicarbonyl on zeolite NaY (Fig. 1).[31] Dealuminated Y zeolite may be among the most nearly ideal supports for metal complexes, but we emphasize that the available samples are not close to being perfectly crystalline (defect free), and even with these supports, the structures of the supported species are somewhat simplified models.

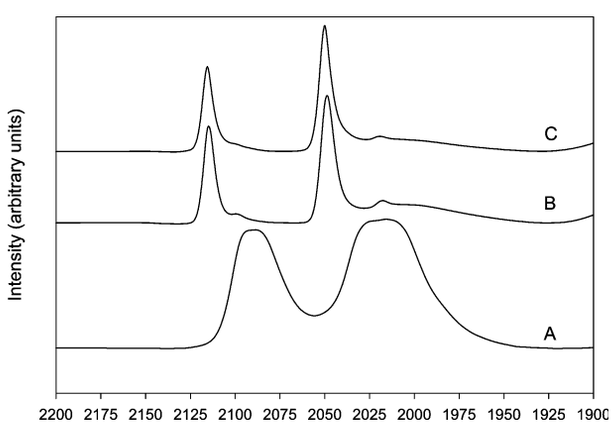

Fig. 1 IR spectra in the carbonyl stretching region of Y zeolite-supported $Rh(CO)_2$: (A) zeolite NaY calcined at 473 K; (B) dealuminated zeolite Y calcined at 393 K; and (C) dealuminated zeolite Y calcined at 573 K.[31]

The implication of near uniformity of structure of $Rh(CO)_2$ in dealuminated zeolite Y (Fig. 2) is that the bonding positions for the metal complex are nearly equivalent crystallographically; thus, the ν_{CO} spectra provide information about the symmetry of the support sites that are ligands in the complex. The IR spectra of the rhodium dicarbonyl represented in Fig. 1 are consistent with a square-planar complex (formally Rh(I)) with the Rh atom bonded to two zeolite oxygen atoms. EXAFS data confirm the presence of approximately 2 CO ligands per Rh atom and approximately 2 support oxygen atoms per Rh atom in the structure, consistent with IR evidence of the symmetry (Table 1, Fig. 1). Calculations at the density functional level, with a fragment (cluster) of the zeolite chosen as the ligand to represent the support, gave structure parameters for $Rh(CO)_2\{OM'\}_2$ (where M′ is Si or Al of the zeolite, Fig. 3) that are consistent with the IR and EXAFS data (Table 1) and the simplified structural model of Fig. 2. It was concluded that

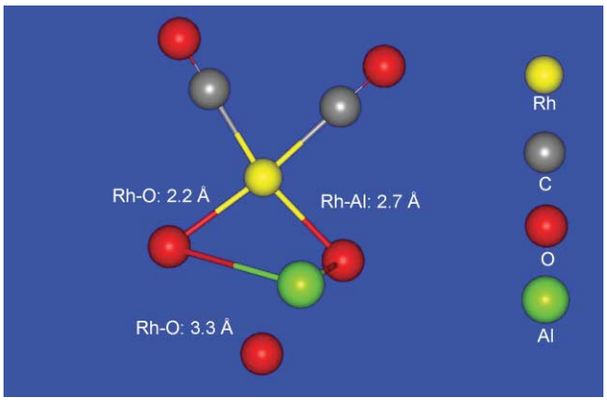

Fig. 2 Simplified structural model of $Rh(CO)_2$ supported in dealuminated Y zeolite developed on the basis of EXAFS data. The figure is not meant to represent bond angles accurately, as such information is not available from the EXAFS data.[31]

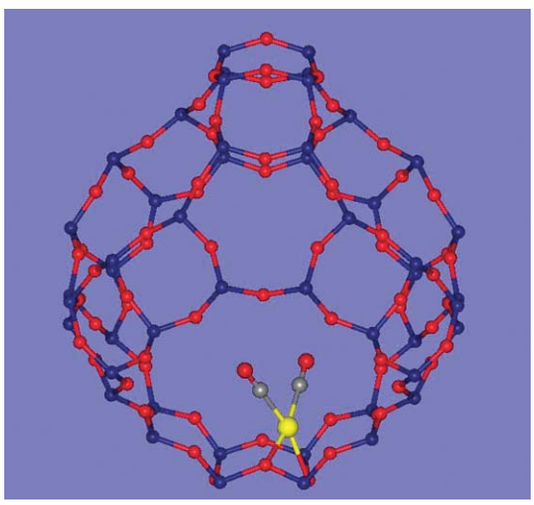

Fig. 3 Structural model representing the location of a rhodium dicarbonyl complex at a faujasite four-ring.[31]

the only sites for bonding of the rhodium complex consistent with all the results are the cation bonding sites shown in Fig. 3 (these are near Al ions in the zeolite). The $Rh^+(CO)_2$ is located at a four-ring of the faujasite framework. The Mulliken charge (the theoretical value of the approximate charge on the Rh atom) was found to be 0.53 e, consistent with the formal designation of the supported species as the 16-electron complex represented as $Rh^I(CO)_2\{OM'\}_2$.

Other thoroughly characterized supported metal complexes include the above-mentioned rhenium tricarbonyls on MgO,[33–35] synthesized from $HRe(CO)_5$, $DRe(CO)_5$, $Re_2(CO)_{10}$, or $H_3Re_3(CO)_{12}$ on the high-area porous powder support[36–38] and separately on MgO films that were hardly more than a monolayer thick and mounted on single crystals of Mo exposing the (110) face.[39] EXAFS data indicate the presence of approximately 3 CO ligands per Re atom and approximately 3 support oxygen atoms per Re atom in the surface structures (Table 1). IR spectra indicate the symmetry and point to two limiting-case structures (Fig. 4).[25,33,34,39,40] The average rhenium tricarbonyl on a largely dehydroxylated MgO powder was found by IR spectroscopy to have approximately three oxygen (O^{2-}) ligands of the support (and C_{3v} symmetry, presuming an octahedral structure). Similarly, the average rhenium tricarbonyl on a hydroxylated MgO powder was found to have approximately three OH ligands of the support.[33] The identification of the ligands in the supported rhenium carbonyls was based on ν_{CO} and ν_{OH} spectra of the samples and molecular analogues. The bands characterizing the carbonyl stretching frequencies from each of the two limiting case structures are clearly distinguishable; the high-frequency carbonyl peaks characteristic of the two structures are separated by 22 cm^{-1}. A partially hydroxylated MgO (with a surface coverage of OH groups of approximately 0.49 monolayer, which corresponds to approximately 1.9 times as many surface OH groups as surface oxygen ions) was postulated to contain mostly $Re(CO)_3\{HOMg\}_2\{OMg\}$.[33]

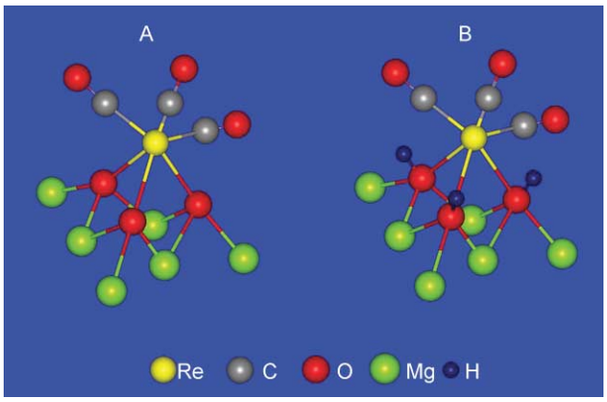

Fig. 4 Models of rhenium tricarbonyl complexes on MgO. (A) $Re(CO)_3\{OMg\}_3$ and (B) $Re(CO)_3\{HOMg\}_3$.[40]

Structural data characterizing samples represented predominantly as $Re(CO)_3\{OMg\}_3$, $Re(CO)_3\{OMg\}_2\{HOMg\}$, $Re(CO)_3\{OMg\}\{HOMg\}_2$, and $Re(CO)_3\{HOMg\}_3$, determined by IR spectroscopy, are summarized in Table 2 (the two limiting structures are shown in Fig. 4). The supported rhenium carbonyls have been characterized by a number of complementary methods, including temperature-programmed decomposition and reduction (which confirm the composition) and Raman, ultraviolet-visible, and inelastic electron tunneling spectroscopies.[34,35,41]

Calculations at the density functional level by the Rösch group,[40] with a fragment of the MgO chosen as the ligand to represent the support (Fig. 4), gave structure parameters for $Re(CO)_3\{OMg\}_3$ bonded at a corner cation defect site of MgO, in good agreement with experimental results characterizing the sample represented as approximately $Re(CO)_3\{OMg\}_2\{HOMg\}$ (Table 3). The $Re–O_s$ distance (the subscript refers to the shorter of the Re–O distances, 2.15 ± 0.03 Å, determined by EXAFS spectroscopy) agrees well with the theoretical value of 2.15 Å for $Re(CO)_3\{OMg\}_3$ (Fig. 4, Table 3). The supported complexes are formally coordinatively saturated (18-electron), and the Re–backscatterer distances and symmetries indicate that they are close analogues of molecular species.[40] The theoretical results show that the $Re–O_s$ bond energy in $Re(CO)_3\{OMg\}_3$ (3.5 eV) is greater than the Re–CO bond energy (2.4–2.5 eV), confirming the role of the oxide support as a strongly bonded tridentate ligand. Many supported metal complexes are strongly bonded to oxide and zeolite supports.

Rhenium tricarbonyls have also been formed on dealuminated zeolite Y, with rhenium inferred to be bonded to three surface oxygen atoms at a T5 site located at an aluminium center in the zeolite, with two oxygen atoms at a four-ring site and one at a six-ring site (Fig. 5).[42] This sample is characterized by sharp ν_{CO} IR spectra, pointing to the uniqueness of the structure and bonding site. Two Re–support oxygen distances were found by EXAFS spectroscopy, 2.09 and 2.47 Å, consistent with Fig. 5. The Re–C and Re–carbonyl oxygen distances were found to be 1.96 and 3.14 Å, respectively. As this appears to be one of the simplest and most uniform supported metal complexes, it would be helpful to investigate its structure and bonding theoretically.

Atomic and molecular species such as CO, Xe, NH_3, NO, O_2, pyridine, and CH_4 have been used frequently as probes of surfaces of oxides and zeolites, with their spectra being used to infer properties of the surface sites to which they bond. The results presented above show that mononuclear metal carbonyls should be added to the list of sensitive probes of these surfaces.

Table 1 Summary of supported mononuclear metal complexes with structures determined by EXAFS spectroscopy[a]

Support	Precursor	Formal oxidation state of metal in precursor	Method of preparation	M–$O_{support}$		M–ligand contributions: M–C		M–ligand contributions: M–O*		Model of surface species	Ref.
				N	*R*/Å	*N*	*R*/Å	*N*	*R*/Å		
MgO calcined at 673 K	$Au(CH_3)_2(C_5H_7O_2)$	3	Adsorption from pentane	2.1	2.16	–	–	–	–	$Au(CH_3)_2\{OMg\}_2$	62
γ-Al_2O_3 calcined at 673 K	$Os_3(CO)_{12}$	0	Decarbonylation in He at 423 K followed by treatment with CO at 473 K	2.9	2.17	2.4	1.93	3.1	3.04	$Os(CO)_3\{OAl\}_3$	46
γ-Al_2O_3 calcined at 673 K	$Os(CO)_3\{OAl\}_3$	2	Oxidative fragmentation in vacuum at 573 K	3.9	2.17	2.0	1.85	2.4	3.04	$Os(CO)_2\{HOAl\}\{OAl\}_3$	46
γ-Al_2O_3 calcined at 673 K	$Os_3(CO)_{12}$	0	Oxidative fragmentation in He at 423 K	3.0	2.17	2.8	1.91	2.8	3.05	$Os(CO)_x\{OAl\}_3$ (mixture of $Os(CO)_2$ and $Os(CO)_3$)	43
γ-Al_2O_3 calcined at 573 K	$Ru_3(CO)_{12}$	0	Oxidative fragmentation in He at 423 K	1.8	2.17	1.8	1.9	2.0	2.97	$Ru(CO)_2\{OAl\}_2$	44
SiO_2 calcined at 433 K	$Ru_3(CO)_{12}$	0	Oxidative fragmentation in air at 298 K	4.9	2.08	2.0	1.87	2.0	3.01	$Ru(CO)_2\{OSi\}_x$	45
DAY zeolite calcined at 393 K	$Rh(CO)_2(acac)$	1	Adsorption from hexane	1.8	2.16	2.3	1.86	2.2	2.97	$Rh(CO)_2\{OAl\}\{OSi\}$	31
DAY zeolite calcined at 573 K	$Rh(CO)_2(acac)$	1	Adsorption from hexane	1.9	2.15	2.2	1.86	2.3	2.96	$Rh(CO)_2\{OAl\}\{OSi\}$	31
γ-Al_2O_3 not calcined	$RhCl_3$	3	Reduction with H_2 at 593 K followed by interaction with CO at 298 K	3.1	2.12	1.8	1.80	1.8	3.00	$Rh(CO)_2\{OAl\}_x$	102
MgO calcined at 973 K	$H_3Re_3(CO)_{12}$	1	Oxidative fragmentation in He or vacuum at 498 K	2.7	2.15	3.0	1.88	3.0	3.09	$Re(CO)_3\{OMg\}_3$	36
										subcarbonyls not completely isolated from each other	37
MgO calcined at 973 K	$HRe(CO)_5$	1	Decarbonylation with H_2 at 353 K	2.8	2.13	3.0	1.91	3.2	3.12	$Re(CO)_3\{OMg\}_x$	37,38
MgO calcined at 673 K	$HRe(CO)_5$	1	Decarbonylation with H_2 at 353 K	2.8	2.13	3.3	1.87	3.1	3.11	$Re(CO)_3\{OMg\}_x$	38
MgO calcined at 636 K	$Re_4(CO)_{12}(OH)_4$	1	Oxidative fragmentation in vacuum at 498 K	3.1	2.17	3.2	1.90	3.3	3.07	$Re(CO)_3\{OMg\}_x$	35
MgO calcined at 636 K	$Re_2(CO)_{10}$	0	Oxidative fragmentation in vacuum at 398 K	3.1	2.18	2.8	1.88	2.9	3.08	$Re(CO)_3\{OMg\}_x$	35
MgO calcined at 523 K	$DRe(CO)_5$	1	Decarbonylation with H_2 at 353 K	2.5	2.16	2.8	1.88	3.0	3.09	$Re(CO)_3\{OMg\}_x$	35
MgO calcined at 523 K	$DRe(CO)_5$	1	Exposure to CH_3OH-saturated He at 423 K	3.1	2.13	2.8	1.85	2.8	3.07	$Re(CO)_3\{OMg\}_x$	35
SiO_2 calcined at 773 K	$Zr(Np)_4$ (Np = neopentyl)	4	Adsorption from pentane	1.1	1.96	3.2 2.8	2.22 3.42	–	–	$Zr(Np)_3\{OSi\}$	48
SiO_2 calcined at 773 K	$Zr(Np)_4$	4	Treatment with H_2 at 423 K	3.1 1.1	1.95 2.61	–	–	–	–	$ZrH\{OSi\}_3$	48
SiO_2 calcined at 773 K	$Ta[CH_2C(CH_3)_3]_3$ $[=CHC(CH_3)_3]$	5	Treatment with H_2 at 298 K	2.3 0.7	1.89 2.63	–	–	–	–	$TaH\{OSi\}_2$	47,48

[a] Notation: *N*, coordination number; *R*, distance between absorber and backscatterer atoms; DAY, dealuminated zeolite Y.

Table 2 Summary of structural assignments and infrared spectra of rhenium carbonyls on MgO[33]

Structural model	Precursor	MgO pre-treatment temperature/K	Molar ratio		Symmetry indicated by IR spectrum	ν, frequency of high-frequency carbonyl band/cm^{-1}	$\Delta\nu$[b] /cm^{-1}	$\Delta\nu/(\Delta\nu)_{max}$	$\left(\frac{N_{O^{2-}}}{N_{OH^-}+N_{O^{2-}}}\right)^c$
			OH^-/O^{2-}	H^+/ Re[a]					
$Re(CO)_3\{OMg\}_3$	$Re_2(CO)_{10}$	973	0.06[d]	0	C_{3v}	2036	22	1.00	1.00
$Re(CO)_3\{OMg\}_2\{HOMg\}$	$H_3Re_3(CO)_{12}$	973	0.06[d]	1	C_s	2028	14	0.64	0.67
$Re(CO)_3\{OMg\}\{HOMg\}_2$	$Re_2(CO)_{10}$	673	1.86[d]	$\geqslant 1$	C_s	2022	8	0.36	0.33
$Re(CO)_3\{HOMg\}_3$	$Re_2(CO)_{10}$	663	$\geqslant 1$[d]	$\geqslant > 1$	C_{3v}	2014	0	0.00	0.00

[a] Determined by composition of precursors. [b] Relative to $Re(CO)_3\{HOMg\}_3$. [c] Fraction of noncarbonyl ligands which are O^{2-} in the complex. [d] Estimated from literature based on MgO pretreatment temperature.

Fig. 5 Structural model of rhenium tricarbonyl supported on dealuminated zeolite Y at a T5 site located at an aluminium center in the zeolite, with two oxygen atoms at a four-ring site and one at a six-ring site.

The supported rhenium carbonyls incorporate Re(I) in a d^6 electronic configuration; with three CO ligands and three surface oxygen ligands, each is a coordinatively saturated 18-electron complex and a probe of three-fold surface sites. The aforementioned $Rh(CO)_2$ complexes incorporate Rh(I) with a d^8 electronic configuration; these stable coordinatively unsaturated 16-electron complexes probe two-fold surface sites. Osmium and ruthenium carbonyls typically exist as either di- or tri-carbonyls and probe surface sites incorporating either three or four oxygen atoms,[43–45] as discussed below.

2.4. Reactivity

Reactivities of supported metal complexes are comparable to those of metal complexes in solution, with a major difference being that some of the ligands in the supported species are provided by the support, the reactivity of which is limited sterically because it is part of a relatively rigid three-dimensional structure (this rigidity is greater for inorganic solids than for organic polymers, and the rigidity of polymers can be regulated, for example, by the crosslink density). The examples given in the next paragraphs illustrate the role of the support as a ligand.

An early example was provided by Deutsch *et al.*,[46] whose EXAFS data showed that when a mononuclear osmium tricarbonyl bonded to γ-Al_2O_3 (formed by the reaction of $Os_3(CO)_{12}$ with γ-Al_2O_3 that had been treated in O_2 at 673 K) was decarbonylated (by treatment in vacuum at 573 K), the number of support oxygen ligands increased by one (the surface switched from a tridentate to a tetradentate ligand) as the number of CO ligands decreased by one; coordinatively saturated species were observed in both cases (Fig. 6).

Another example illustrating the role of the support is provided by silica-supported tantalum complexes. The reaction of the carbene complex $Ta(=CHC(CH_3)_3)(CH_2C(CH_3)_3)_3$ with SiO_2 that had been calcined at 773 K leads to formation of silica-supported complexes [$\{SiO\}$–$Ta(=CHC(CH_3)_3)(CH_2C(CH_3)_3)_2$ and $\{SiO\}_2Ta(=CHC(CH_3)_3)(CH_2C(CH_3)_3)$ with a ratio of roughly 65 : 35] that, upon treatment in H_2 at 298 K, gives a supported tantalum hydride, inferred from EXAFS and IR spectra to be $HTa\{OSi\}_2$ (Fig. 7).[47] Related work has been reported for hydrides of Ti, Zr, and Hf on silica.[48]

The bonding of these tantalum complexes to SiO_2 surfaces that had been treated at various temperatures (573, 773, and 973 K) to control the density of surface silanol and siloxane groups was reported.[49] When the surface concentration of silanol groups was about 0.01 per Å^2 (in SiO_2 calcined at 973 K), the reaction gave predominantly $\{SiO\}$–Ta(=CHC-

Table 3 Calculated properties of $Re(CO)_3\{OMg\}_3$ and $Re(CO)_3\{HOMg\}_3$ compared with experimental results[a 40]

Structure	*r*(Re–O)	*r*(Re–C)	*r*(C–O)	*r*(Re–Mg1)	*r*(Re–Mg2)	E_b	*ν*(Re–MgO)	*ν*(Re–CO)
$Re(CO)_3\{OMg\}_3$								
$Re^0(CO)_3/V_s^-$	2.26	1.90	1.18	2.03	2.02	2.79	528	510
$Re^I(CO)_3/V_s^-$ [b]	2.15	1.95	1.16	2.04	2.09	3.51	552	479
$Re^I(CO)_3/V_s$	2.05	2.02	1.15	2.05	2.15	2.74	551	439
Experiment[c]	2.15	1.88						
$Re_3(CO)_3\{HOMg\}_3$								
$Re^I(CO)_3/V_s(OH)$	2.55	1.91	1.17	2.03	2.07	0.67	417	523

[a] Distances *r* in Å, binding energy E_b of $Re(CO)_3$ species to MgO in eV per Re–O bond (of three bonds), vibrational frequencies *ν* in cm^{-1}; V_s refers to surface defect site. Refer to Fig. 4 for structures of $Re(CO)_3\{OMg\}_3$ and $Re(CO)_3\{HOMg\}_3$. Mg1 and Mg2 refer to the first and second nearest Mg atom to the Re atom, respectively. [b] Also represents $Re^0(CO)_3/V_s$ where E_b = 3.37 eV per Re–O bond with respect to $Re(CO)_3$ and $\{OMg\}_3$ (V_s). [c] Experimental distance from EXAFS spectroscopy for structure approximated as $Re_3(CO)_3\{OMg\}_2\{HOMg\}$.[33,35]

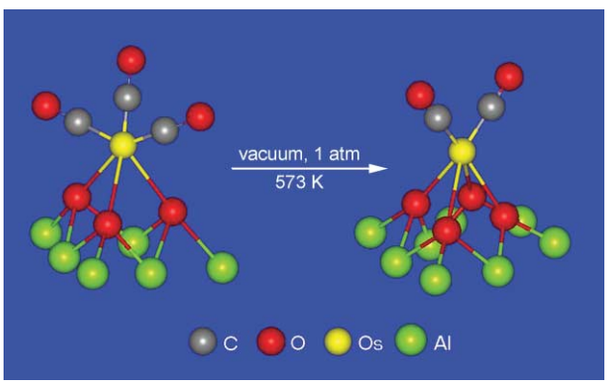

Fig. 6 Structural model of the partial decarbonylation of a mononuclear osmium tricarbonyl bonded to γ-Al_2O_3. The number of support oxygen ligands increased by one as the number of CO ligands decreased by one.[46]

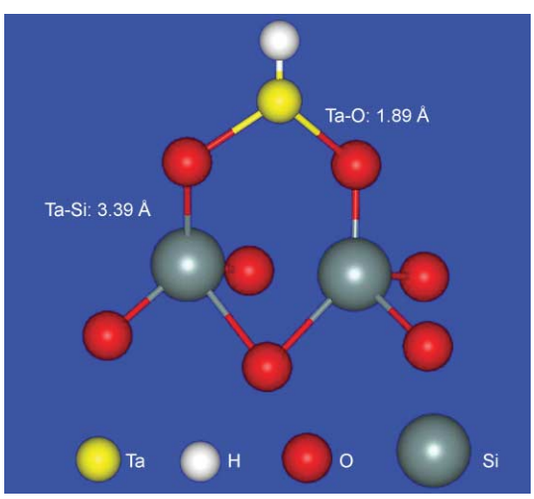

Fig. 7 Simplified structural model of tantalum hydride supported on SiO_2 determined from IR, NMR, and EXAFS data.

$(CH_3)_3)(CH_2C(CH_3)_3)_2$ with one covalent bond to the silica support, but when the surface concentration of these groups was about 0.04 per Å² (in SiO_2 calcined at 573 K), the predominant surface species was $\{SiO\}_2Ta(=CHC(CH_3)_3)(CH_2C(CH_3)_3)$, which is anchored by two covalent bonds to silica.

The results show that only one Si–OH group in the highly dehydroxylated silica (with a surface area of 200 $m^2\ g^{-1}$) can be present in the area covered by an adsorbed complex derived from the tris(neopentyl)neopentylidene tantalum, which has an estimated projected area of 90 Å², when the tantalum content of the sample is about 6 wt% Ta (*i.e.*, 330 μmol of Ta per gram of SiO_2). The results show that about 90% of the dehydroxylated silica surface is covered by $\{SiO\}$–$Ta(=CHC(CH_3)_3)(CH_2C(CH_3)_3)_2$. The density of Si–OH groups in the hydroxylated silica is greater, allowing the interaction of two nearby silanol groups with the tantalum complex; these complexes cover about 60% of the silica surface.

Metal complexes on supports can in prospect be made to be coordinatively unsaturated; the bonding to the support may hinder the interactions of neighboring complexes with each other and thereby stabilize the coordinative unsaturation and allow catalytic activity (in contrast to the dimerization or aggregation of coordinativley unsaturated species that may occur readily in solution and lead to coordinatively saturated and catalytically inactive species).

IR spectra show that when the above-mentioned silica-supported tantalum complexes formed by the reaction of $Ta(=CHC(CH_3)_3)(CH_2C(CH_3)_3)_3$ with hydroxyl groups of SiO_2 that had been calcined at various temperatures (a mixture of $\{SiO\}$–$Ta(=CHC(CH_3)_3)(CH_2C(CH_3)_3)_2$ and $\{SiO\}_2Ta(=CHC(CH_3)_3)(CH_2C(CH_3)_3)$, depending on the degree of surface hydroxylation[49]) are treated in H_2 at temperatures up to 773 K, the complexes are dehydrogenated, presumably as a hydride is transferred from Ta to Si of the support surface and a siloxy group of the support becomes bonded to the Ta. The reaction was inferred to give $Ta^{III}\{OSi\}_3$ by opening of a Si–O–Si bridge on the silica. The reaction involving a rearrangement of the silica surface seemingly requires a flexibility of the surface that may not be matched by other supports, especially zeolites. The postulated $Ta^{III}\{OSi\}_3$ is remarkable for its degree of coordinative unsaturation,[50] and it may be considered surprising that hydride ligands do not migrate from the silica surface onto the Ta; such complexes are worthy of further investigation.

Miessner[51] showed that partial decarbonylation of the above-mentioned zeolite-supported rhodium dicarbonyl complex by treatment in H_2 at temperatures of 473–523 K leads to coordinatively unsaturated complexes that are so highly reactive that they combine with N_2 to give supported complexes with dinitrogen ligands. This remarkable reactivity suggests possibilities for new catalytic properties of these and related supported metal complexes. Photochemistry may initiate the reaction of alkanes on such complexes.[52]

Many other reactions of supported metal complexes have been investigated, some shown to be similar to those of analogous complexes in solution. Reactions of organic ligands on numerous supported metal complexes have been reviewed recently.[53]

A common reaction of supported complexes of noble metals is reduction of the metal to the zero-valent state, giving clusters or particles. An example is the above-mentioned reaction of $\{SiO\}Rh(allyl)_2$ on silica to give small rhodium particles, observed by transmission electron microscoscopy.[22,54] Some of these processes might be described as auto-reductions, and most are not fully characterized. One should investigate the oxidation state(s) of the metal in supported samples to test for reduction (see below) and examine them by electron

microscopy and EXAFS spectroscopy to check for the presence of clusters or particles.

2.5. Determination of oxidation states of metals

The oxidation states of metals in supported metal complexes can be determined experimentally by temperature-programmed reduction and temperature-programmed oxidation. The methods work well when the reduction or oxidation processes lead to metal complexes or clusters with the metals in unique oxidation states. An example of the characterization of a supported metal complex by temperature-programmed methods is provided by MgO-supported gold complexes prepared by the reaction of $Au^{III}(CH_3)_2(C_5H_7O_2)$ with MgO that had been partially dehydroxylated by evacuation at 673 K. When the resultant surface species, $Au^{III}(CH_3)_2\{OMg\}_2$ (identified by IR and EXAFS spectroscopies), was reduced by treatment in H_2, the H_2 uptake was 1.51 ± 0.05 mol of H_2 per Au atom, consistent with the reduction of Au(III) to metallic gold in the form of clusters (indicated by EXAFS spectroscopy). Similarly, metallic gold clusters could be oxidized to Au(III).[55]

These data are by themselves not sufficient to characterize the oxidation and reduction processes fully, but when they are combined with results from X-ray absorption near edge spectroscopy (XANES) the redox process may be well characterized. These changes were characterized qualitatively by XANES[56] and quantitatively by temperature-programmed reduction and temperature-programmed oxidation; XANES[55] allows one to distinguish between Au(0), Au(I), and Au(III), and so XANES in combination with quantitative results from the temperature-programmed oxidation and reduction allows a full characterization of the oxidation states of supported gold.

This example is, however, not typical, because for many supported metal complexes XANES is not sufficient to determine the oxidation states of the metal, especially when there are mixtures. Rhodium complexes on γ-Al_2O_3, for example, may be present with the metal in the 0, 1+, and 3+ oxidation states, but the XANES spectra are too complex to distinguish them and sometimes do not even show clearly which ones are present.[57] X-Ray photoelectron spectroscopy can be helpful, but the results are affected by the degree of aggregation of the metal and are often not unequivocal either.

2.6. Catalysis

Alkane metathesis. The metathesis reaction of linear or branched alkanes catalyzed by silica-supported transition metal hydrides to form the next higher and lower alkanes under mild conditions (300 K and atmospheric pressure) was discovered recently.[18,47,58,59] In contrast to the well-investigated alkene metathesis reaction whereby alkylidene fragments are exchanged, in this new reaction, alkyl fragments of alkanes were suggested to be exchanged. It was suggested that the key steps in the reaction mechanism are a) activation of a C–C bond of an alkane on the surface tantalum complex, leading to the evolution of an alkane and the formation of a new surface complex and b) regeneration of the tantalum complex in an alkyl-exchange reaction (C–H bond activation).

Polyalkene hydrogenolysis. Basset's group[17,60] showed that silica-supported complexes of Hf and Zr catalyze polyalkene hydrogenolysis—potentially a route to environmentally friendly conversion of waste plastics into the monomers. This new catalytic reaction has been suggested to proceed by successive β-alkyl transfer (in the C–C bond cleavage) and hydrogenolysis steps. The suggested β-alkyl transfer step corresponds to the reverse of the insertion of an alkene into a metal–carbon bond.[61]

Hydrogenation of ethene catalyzed by a gold complex. The above-mentioned mononuclear gold complex prepared on MgO formed from $Au(CH_3)_2(C_5H_7O_2)$ and represented on the basis of IR and EXAFS spectra as $Au^{III}(CH_3)_2\{OMg\}_2$ is the precursor of a catalyst for ethene hydrogenation;[62] the rate of the catalytic reaction at 353 K and atmospheric pressure in the presence of a mixture of ethene, H_2, and He (ethene partial pressure, P_{ethene}, 40 Torr; $P_{hydrogen}$, 160 Torr) was found to be 2.9×10^{-3} molecules of ethene (Au atom × s)$^{-1}$. Formation of ethene-derived adsorbates (ethyl and π-bonded ethene) on the gold center was observed by IR spectroscopy during catalysis, and EXAFS spectra indicated that the gold was present in isolated mononuclear complexes; the mononuclear gold complexes themselves were inferred to be the catalytically active species.[62]

3. Chemistry of supported metal clusters

3.1. Synthesis

Methods for the synthesis of supported metal clusters include bonding of precursor metal carbonyl clusters (or reaction of precursors to form metal carbonyl clusters on the support), followed by removal of carbonyl ligands. This and related methods are reviewed elsewhere,[5,63] and only a few details are repeated here.

For example, metal carbonyl clusters (*e.g.*, $Ir_4(CO)_{12}$, $Ir_6(CO)_{16}$, and $Rh_6(CO)_{16}$) are adsorbed intact from solution (*e.g.*, *n*-pentane) onto more-or-less neutral supports such as γ-Al_2O_3 or TiO_2. When such clusters are adsorbed on basic supports such as MgO or La_2O_3, surface anions are typically formed (*e.g.*, $[HIr_4(CO)_{11}]^-$ and $[Ir_6(CO)_{15}]^{2-}$ from $Ir_4(CO)_{12}$ and $Ir_6(CO)_{16}$, respectively).

Alternatively, supported metal carbonyl clusters are formed by surface-mediated synthesis from mononuclear metal complexes (examples are $[HIr_4(CO)_{11}]^-$ formed from $Ir(CO)_2$(acac) on MgO and $[Rh_5(CO)_{15}]^-$ formed from $Rh(CO)_2$(acac) on MgO and γ-Al_2O_3 in the presence of CO and in the absence of solvents).[64,65] Synthesis of metal carbonyl clusters on oxide supports apparently often involves OH groups or water on the support surface; analogous chemistry occurs in solution.[6,63] The synthesis from a mononuclear metal complex is likely to occur with a yield less than that associated with simple adsorption of a preformed metal cluster, and so the latter precursors are preferred, except when they do not fit into the pores of the support (*e.g.*, a zeolite).

Sometimes the solvent-free synthesis of metal carbonyl clusters on oxide surfaces (followed by extraction into a solvent) is a more convenient and efficient method to prepare the clusters than conventional syntheses in solution. Surface-mediated synthesis of metal clusters has developed into a lively field in its own right.[66,67]

Quantitative characterization of the formation of $[Os_5C(CO)_{14}]^-$ from a smaller precursor on MgO was characterized by ^{13}C NMR spectroscopy.[68] The multistep synthesis from $Os_3(CO)_{12}$ gave $[Os_5C(CO)_{14}]^-$ in a yield of about 65%; other products included tri- and tetra-osmium carbonyl clusters. The latter clusters on MgO have been observed by high-resolution transmission electron microscopy (Fig. 8).[69]

Supported metal carbonyl clusters such as $[Os_5C(CO)_{14}]^{2-}$, $Ir_4(CO)_{12}$, and $Rh_6(CO)_{16}$ are themselves of limited interest in our context because most attempts to do chemistry on them lead to a loss of structural simplicity of the metal-containing species; for example, treatments intended to remove the CO ligands from clusters such as $Ir_4(CO)_{12}$ and $Rh_6(CO)_{16}$ usually lead to mixtures of clusters of various sizes and/or cationic complexes of the metal formed by oxidative fragmentation (support OH groups may facilitate this reaction).[19]

Early interest in forming uniform de-ligated clusters on supports was strong, because these materials provide a link between molecular metal clusters and the (non-uniform) metal entities in conventional supported metal catalysts,[70] but the

Table 4 Structural data determined by X-ray diffraction for individual organometallic compounds that are analogues of supported metal complexes

Structural formula	M–O average distance/Å	Formal oxidation state of metal	Reference
$[Ru(CO)_2(OCOCF_3)(\mu\text{-}OSiMe_2CH_2PPh_2)]_2$	2.14	2	76
$[OsH(\eta^2\text{-}O_2)(dcpe)_2]^{+}$ [a]	2.05	2	77
$CF_3CO_2W(CO)_2(\pi\text{-}C_3H_5)(CH_3O(CH_2)_2OCH_3)$	2.09 [b]	2	78
	2.25 [c]		
$[[(C_7H_8)Rh]_5(Nb_2W_4O_{19})_2]^{3-}$	2.10	1	79
$[(CO)_3W(\mu\text{-}OH)_3W(CO)_3]^{3-}$	2.16	0	80
$W[C_3(CMe_3)Et_2](O_2CCH_3)_3$	2.17	4	81
$W(CO)(C_5Me_5)(O_2CCF_3)_2[\eta^2\text{-}C(O)C_2H_4CO_2Me]$	2.12	4	82
$[[(C_8H_{12})Ir]_2H(Nb_2W_4O_{19})_2]^{5-}$	2.00	1	83
$[(C_7H_8)Rh(P_3O_9)]^{2-}$	2.27 [d]	1	84
$[Re(CO)_3(\mu_3\text{-}OH)]_4$	2.21	1	85
$[(CO)_3Re(\mu\text{-}OCH_3)_3Re(CO)_3]^{-}$	2.08	1	86
$[(CO)_3Re(\mu\text{-}OC_6H_5)_3Re(CO)_3]^{-}$	2.14	1	87
$[(C_8H_{12})Ir(P_3O_9)]^{2-}$	2.18 [e]	1	83
	2.70 [f]		
$[(C_8H_{12}O)Ir(P_3O_9)]^{2-}$	2.12 [g]	3	88
$[(C_8H_{11}OH)Ir(P_3O_9)]^{2-}$	2.20	3	88

[a] dcpe = 1,2-bis(dicyclohexylphosphino)ethane. [b] Trifluoroacetate ligand. [c] Dimethoxyethane ligand. [d] The distorted M–O bond distance is probably a result of a structural compromise between square-pyramidal and trigonal-bipyramidal geometry at rhodium and is included for completeness. [e] Basal plane. [f] Apical site. [g] Oxametallocyclobutane ligand.

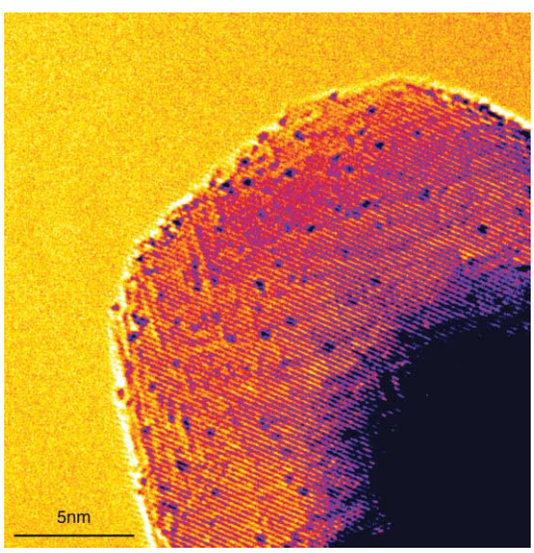

Fig. 8 High-resolution transmission electron micrograph of $[Os_5C(CO)_{14}]^{2-}$ on MgO. This cluster was present with osmium carbonyl clusters with lower nuclearities (containing three and four Os atoms).[69]

interest rapidly waned as it became clear that most synthetic approaches led to non-uniform samples. Persistent experimentation showed, however, that high yields of structurally simple supported clusters such as Ir_4, Ir_6, Rh_6, and Os_5C could be prepared by mild decarbonylation of supported precursors such as $Ir_4(CO)_{12}$ (or $[HIr_4(CO)_{11}]^{-}$), $Ir_6(CO)_{16}$ (or $[Ir_6(CO)_{15}]^{2-}$), $Rh_6(CO)_{16}$, or $[Os_5C(CO)_{14}]^{2-}$, respectively.[63] Trial-and-error experimentation determined the conditions of the decarbonylations. Characterization of these samples is challenging, and the yields are not determined as quantitatively as one would wish. These samples are considered in the following paragraphs.

The decarbonylation of supported metal carbonyl clusters sometimes occurs almost without changes in the metal frame of the cluster, but the chemistry is only partially understood. When decarbonylation takes place at elevated temperatures (depending on the support), migration and aggregation of the metal occur.

When $[HIr_4(CO)_{11}]^{-}$ on MgO, for example, was treated in He at 573 K, the CO ligands were removed fully, as shown by IR and EXAFS spectra, and the Ir_4 tetrahedra remained essentially intact, as shown by EXAFS spectra.[63,71] IR spectra indicated the formation of formate and carbonate on the MgO.[71] When the decarbonylation took place in the presence of H_2, the iridium more readily aggregated into larger clusters. Similar results pertain to the decarbonylation of neutral clusters of Ir and of Rh and to anionic clusters of these metals in addition to $[HIr_4(CO)_{11}]^{-}$.[6,63] The decarbonylation of oxide-supported metal carbonyls yields gaseous products including not just CO, but also CO_2 and H_2.[72] The decarbonylation chemistry involves the support surface and breaking of C–O bonds and has been thought to possibly leave C on the clusters.[73] The chemistry seems to bear some relationship to that occurring in Fischer–Tropsch catalysis on metal surfaces.[72]

When $Ir_4(CO)_{12}$ was present in the cages of zeolite NaY, it was decarbonylated by treatment in H_2 at 573 K.[74] This cluster could not be reconstructed by simple treatment in CO, but when the sample was cooled to liquid nitrogen temperature and treated in CO, IR spectra indicated that the iridium clusters were oxidatively fragmented, giving structures represented as $Ir(CO)_2$ or $Ir(CO)_3$, and when these were treated in CO as the temperature was raised, they were reconstructed into $Ir_4(CO)_{12}$ at about 323 K. With further increases in temperature this was observed to be converted into $Ir_6(CO)_{16}$ at about 398 K. The chemistry seems to be similar to the solution chemistry of the cluster formation from hydrated $IrCl_3$ in CO under mild conditions (423 K and 1 bar);[75] it is an example of surface-mediated cluster synthesis.

3.2. Bonding of clusters to supports

EXAFS results characterizing metal–oxygen (M–O) contributions in numerous oxide- and zeolite-supported metal clusters (where M is Ru, Rh, Ir, Os, Pt, *etc*.) indicate distances in the range of 2.1–2.2 Å.[26,63] Other metal–oxygen contributions at a distance of typically 2.6 or 2.7 Å (referred to as $M–O_l$ contributions, where l refers to long, in contrast to $M–O_s$, where s refers to short) are also commonly observed for oxide- and zeolite-supported transition metal clusters.[26,63] The shorter ($M–O_s$) distances are bonding distances, essentially matching those in supported metal complexes (*e.g*., Figs. 2–6) and those determined by XRD in molecular metal complexes in which metal ions are bonded to oxygen, exemplified by compounds that are analogues of supported metal complexes, such as $[Ru(CO)_2(OCOCF_3)(\mu\text{-}OSiMe_2CH_2PPh_2)]_2$ and $[Re(CO)_3(\mu_3\text{-}OH)]_4$ (Table 4).[37,76–88]

Density functional theory has been used to characterize the cluster–support interface.[89,90] The results characterizing Ir_4 in

zeolite NaX, for example (assumed to be present at a six-ring, Fig. 9), indicate Ir–O distances of about 2.2 Å, in good agreement with EXAFS data.[90,91] Similarly, theoretical results representing Os_5C on MgO (Fig. 10) indicate Os–O_s distances of about 2.1 Å, in good agreement with the EXAFS data.[90,91] The longer metal–oxygen distances of about 2.6 Å observed by EXAFS spectroscopy for these and related supported metal clusters suggest weak interactions between the metal and surface oxygen atoms; these interactions are not well understood.

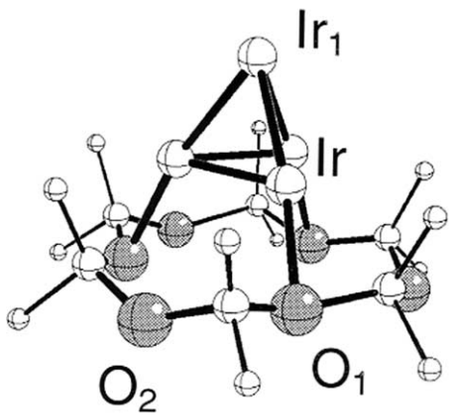

Fig. 9 Model of Ir_4 cluster supported at a six-ring of zeolite NaX.[89]

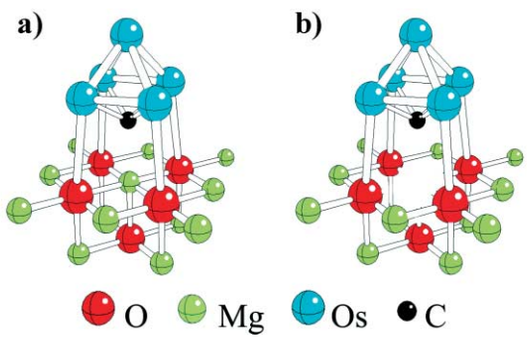

Fig. 10 Models of osmium clusters supported on MgO(001). (a) $Os_5C/Mg_{13}O_5$, and (b) Os_5C at a surface point V_s defect site.[90]

A clear result of the calculations at the density functional level is that the shorter metal–oxygen distances are bonding distances, consistent with the presence of metals bearing positive charges at the metal–support interface. The bonds are rather strong, in line with the theoretical results stated above for supported metal complexes (Table 3), and they explain the stability of extremely small metal clusters on supports. The results confirm the essential agreement between the EXAFS spectra characterizing the shorter metal–oxygen distances in supported mononuclear metal complexes and those in supported metal clusters (even including clusters markedly larger than the ones considered here[91]).

Results characterizing Rh_6 in a faujasite zeolite confirm the inference that the metal atoms in metal clusters and particles at the metal–support interface are positively charged (Fig. 11).[92] The positive charge of the cluster is borne almost entirely by the metal atoms at the metal–support interface; those farther from the interface are essentially uncharged. The theoretical result is consistent with the EXAFS results and the conclusion that supported metal clusters are bonded to the supports by metal–oxygen bonds with distances of about 2.1–2.2 Å[30a] (the value calculated for Rh_6 on the zeolite was 2.2 Å). The Mulliken charge of the Rh atoms at the metal–support interface in Rh_6 on the zeolite was estimated to be 0.76 e. This compares with the Mulliken charge of 0.53 e of the rhodium atom in $Rh(CO)_2$ bonded to zeolite USY (Fig. 3);[31,93] the results are consistent

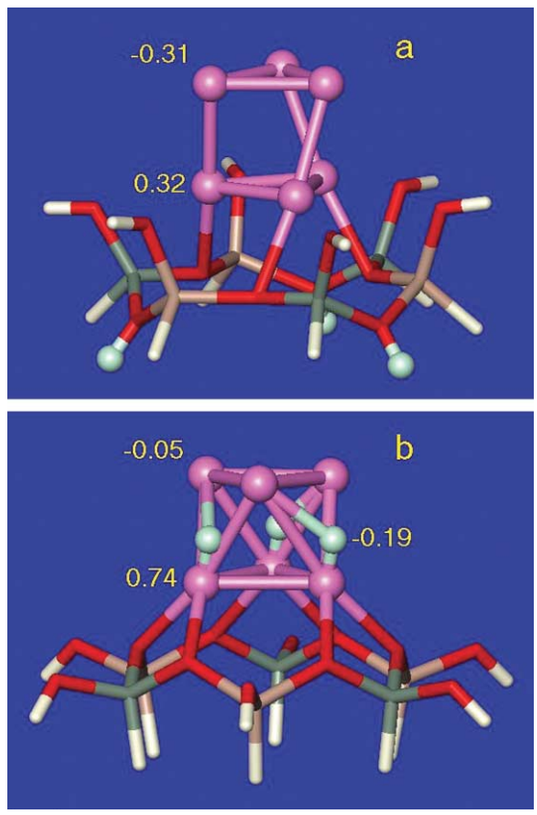

Fig. 11 (a) Model of Rh_6 supported on a zeolite fragment with three bridging OH groups. (b) Model of Rh_6 with three hydride ligands supported on a zeolite fragment formed by reverse spillover of hydrogen from a zeolite fragment with three OH groups. Mulliken charges (in e) of the atoms in the supported cluster are shown.[92]

with the suggestion that the Rh atoms at the interfaces in each sample should be represented formally as Rh(I).

Another example of cationic metal atoms in clusters at the metal–support interface is provided by a sample modeled as trirhenium rafts (formed from $H_3Re_3(CO)_{12}$) on γ-Al_2O_3,[94] with the rhenium atoms being in an oxidation state in the range of about +4 to +6 (as inferred from XANES and X-ray photoelectron spectra). Additional evidence of the cationic character of the rhenium on the surface is provided by the short Re–Re distance (2.67 Å), suggesting a multiple bond. The structure of this sample is not fully understood, but it is intriguing because it is comparable to structures of numerous compounds with cationic metals and short metal–metal bonds and groups bridging them such as polycarbonate anions[95] (which play a role comparable to that of the oxide support).

Calculations were carried out for Os_5C clusters on MgO (Fig. 10); bonding on the stable square (001) face as well as at defect sites was considered. The results indicate that Os_5C is bonded markedly more strongly at surface defect sites than at defect-free sites (Fig. 10). The binding interaction of Os_5C on the MgO(001) surface at a V_s defect site is 4.84 eV greater than the value characterizing the cluster bonded at a defect-free site on the same surface. The results seem likely to be general—metal clusters on metal oxides are expected to be present predominantly at defect sites.[90] (This generalization may extend to mononuclear metal complexes on metal oxides as well.)

3.3. Metal–metal distances and ligands in supported metal clusters

Metal–metal distances in supported metal clusters (*e.g.*, Ir_4, nearly 2.70 Å) determined by EXAFS spectroscopy essentially match those in coordinatively saturated clusters of the same metal (*e.g.*, $Ir_4(CO)_{12}$). These distances are markedly greater (by about 0.2–0.3 Å) than the metal–metal distances in the free

(gas-phase) clusters (*e.g.*, Ir_4, 2.44 Å).[89] Similar results have been determined for supported Os_5C[90] and Rh_6.[92] These comparisons led the Rösch group[89,90] to conclude that some ligands remained on the clusters after decarbonylation; this conclusion may be quite general.[89] The candidate ligands include C (from CO ligands of the precursor) and H (from the support). Calculations by Vayssilov *et al.*[92] for hydride ligands on Rh_6 supported on a faujasite show that they are more strongly bonded than C ligands, and thus it was inferred that the ligands on the clusters are likely to be hydrogen and not carbon; this inference may be rather general for noble metals but needs testing. The calculations showed that Rh_6 on the support (assumed to be at a six-ring of the zeolite, Fig. 11) with H ligands in bridging positions is markedly more stable (by 370 kJ mol^{-1} per cluster) than the bare cluster on the zeolite with OH groups (Fig. 11).

The supported clusters have a strong affinity for the hydride ligands. The process by which protons of the support provide hydride ligands for the metal is called reverse spillover. The opposite process (spillover), well known in catalysis by supported metals,[96] is shown by the theoretical results to be a redox process; in reverse spillover, the support OH groups oxidize the cluster (Fig. 11).

The theoretical and EXAFS results characterizing zeolite-supported Rh_6 raise the question of whether ligand-free clusters (or even ligand-free mononuclear metal complexes) are stable on hydroxylated supports.[92] If reverse spillover to make supported metal hydrides is essentially unavoidable, questions are also raised about the interpretation of chemisorption measurements intended to determine the number of bonding sites of (even conventional) supported metal catalysts, which in typical chemisorption experiments need to be cleaned to remove adsorbates (ligands), usually by evacuation of the sample. Evacuation can remove H_2, at the expense of support OH groups, but questions remain: are the clusters stable during this process, and do their morphologies change?[92]

The commonly characterized ligands on the supported metal clusters mentioned above include CO, hydride, and hydrocarbons. Evidence of hydride is not as strong as one would wish. ^{1}H NMR spectroscopy has been used to detect it on La_2O_3-supported Rh_6,[97] and the kinetics of chemisorption of H_2 supports the inference of hydride formation (by dissociative adsorption of H_2 on Ir_4).[98] Propylidyne formed from propene on Ir_4 supported on γ-Al_2O_3 was observed by IR and ^{13}C NMR spectroscopies.[98]

When ethene or propene was brought in contact with oxide-supported Ir_4, Ir_6, or Rh_6 in the presence of H_2, hydrocarbon ligands were formed, alkyls and π-bonded alkenes, which have been inferred from IR spectra to be intermediates in hydrogenation to make alkanes, as discussed below. Much remains to be done to develop the chemistry of organic ligands on supported metal clusters, and substantial progress is expected as the samples are well suited to characterization by both IR and NMR spectroscopies.

3.4. Stability of supported clusters

The results of EXAFS and density functional theory for supported clusters show that they are anchored to oxides and zeolites through strong bonds, which explains why the clusters have a significant resistance to migration and aggregation (which nonetheless occurs at elevated temperatures). The results of the calculations for a family of osmium clusters on MgO indicate that clusters supported on oxides with defect sites are more stably dispersed than those on surfaces without such sites.[90]

Metal clusters in zeolites have been thought to be stabilized by their confinement in the intracrystalline cages.[99] This is an appealing idea but perhaps not yet sufficiently demonstrated. Under some conditions, metals migrate out of zeolite pores and onto the outside crystallite surfaces,[100] and, under some conditions, metals in zeolite cages expand with sufficient force to burst the structure of the zeolite frame.[101]

Metal clusters on supports may also fragment to give mononuclear metal complexes, as illustrated by the reaction of CO with rhodium clusters supported on γ-Al_2O_3[19,102] and by the reaction of CO with iridium clusters in a zeolite, described above.[74]

3.5. Preparation and characterization of supported bimetallic clusters

When supported catalysts are prepared from precursors such as metal carbonyls incorporating more than one metal, the resultant supported species may be small supported metal clusters.[103,104] When bimetallic clusters incorporating only noble metals are adsorbed on a support and the precursor ligands removed, the resultant species are usually aggregated and non-uniform. However, extremely small PtRu clusters dispersed on γ-Al_2O_3 were prepared by decarbonylation of molecularly adsorbed $Pt_2Ru_4(CO)_{18}$ by treatment in He or H_2 at temperatures in the range of 573–673 K.[105] EXAFS data show that, after decarbonylation, the Pt–Ru interactions were largely maintained, but the Pt–Ru cluster frame was changed. The average Pt–Pt bond distance apparently increased slightly (from 2.66 to 2.69 Å), and the Ru–Ru distance decreased from 2.83 to 2.64 Å. The corresponding Pt–Pt and Ru–Ru coordination numbers were found to be 2.0 and 4.0, respectively, indicating that slight agglomeration of the metal took place, and the clusters incorporated, on average, less than three and six Pt and Ru atoms, respectively, being the smallest supported bimetallic clusters of platinum-group metals yet reported.

When a supported metal on an oxide is prepared from an adsorbed precursor incorporating a noble metal bonded to an oxophilic metal, the result may be small noble metal clusters, each more-or-less nested in a cluster of atoms of the oxophilic metal, which is oxidized and anchored to the support through metal–oxygen bonds.[106,107] The simplest such structure appears to be well approximated as Re_4Pt_2, made from $Re_2Pt(CO)_{12}$; EXAFS data led to the postulate of a surface species in which rhenium interacts strongly with the oxygen atoms of the support and also with platinum (Fig. 12).[108] When one of the metals in a supported bimetallic cluster is noble and the other oxophilic, the oxophilic metal interacts more strongly with the support than the noble metal; if the bimetallic frame of the precursor is maintained nearly intact, then this metal–support interaction helps keep the noble metal highly dispersed. Other samples of such "nested" noble metal clusters on oxides have been made from the following precursors: $Pd_2Mo_2(CO)_6(C_5H_5)_2(PPh_3)_2$,[106] $PtMo_2(CO)_6(C_5H_5)_2(PhCN)_2$,[107] $PtW_2(CO)_6(C_5H_5)_2(PhCN)_2$,[109] $Pt_2W_2(CO)_6(C_5H_5)_2(PPh_3)_2$,[110] and $[Ru_{12}C_2Cu_4Cl_2(CO)_{32}][PPN]_2$,[111] among others. Platinum clusters of as few as four atoms each, on average, are indicated by EXAFS data characterizing the Pt–W clusters.[110] The Pt–W samples, for example, are remarkably stable, with the cluster size remaining essentially unchanged after oxidation–reduction cycles at

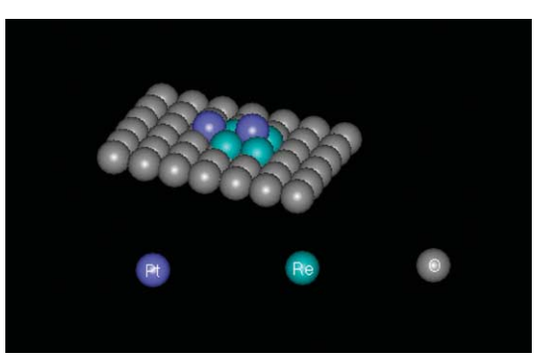

Fig. 12 Simplified model based on EXAFS data of Re_4Pt_2 clusters formed on the surface of γ-Al_2O_3 from $Re_2Pt(CO)_{12}$.[108]

Table 5 EXAFS structural parameters of supported metal clusters during exposure to various reactive atmospheres and during propene hydrogenation catalysis at 298 K and 1 atmosphere[a]

	Conditions during scan				EXFAS parameters	
Catalyst modeled as	$P_{propene}$/bar	$P_{hydrogen}$/bar	$P_{nitrogen}$/bar	Contribution	*N*	*R*/Å
$Ir_4/\gamma\text{-}Al_2O_3$	0.0	0.0	1.0	Ir–Ir	3.2	2.67
				Ir–O	1.3	2.17
	0.0	1.0	0.0	Ir–Ir	3.2	2.71
				Ir–O	1.3	2.17
	1.0	0.0	0.0	Ir–Ir	3.1	2.70
				Ir–O	1.3	2.17
	0.5	0.5	0.0	Ir–Ir	3.2	2.71
				Ir–O	1.3	2.17
$Ir_6/\gamma\text{-}Al_2O_3$	0.0	0.0	1.0	Ir–Ir	3.9	2.70
				Ir–O	1.3	2.26
	0.0	1.0	0.0	Ir–Ir	4.0	2.71
				Ir–O	1.3	2.23
	1.0	0.0	0.0	Ir–Ir	4.1	2.70
				Ir–O	1.0	2.21
	0.5	0.5	0.0	Ir–Ir	4.0	2.71
				Ir–O	1.3	2.23
Ir_4/MgO	0.0	0.0	1.0	Ir–Ir	3.0	2.67
				Ir–O	1.3	2.15
	0.0	1.0	0.0	Ir–Ir	2.9	2.70
				Ir–O	1.3	2.15
	1.0	0.0	0.0	Ir–Ir	3.2	2.71
				Ir–O	1.5	2.15
	0.5	0.5	0.0	Ir–Ir	3.0	2.72
				Ir–O	1.3	2.15

[a] Notation: *N*, coordination number, *R*, distance between absorber and backscatterer atom. Adapted from ref. 112.

673 K.[109,110] The stability is attributed to the nesting by the oxophilic metals. The stability of these samples could be a significant advantage in catalytic applications.

3.6. Catalysis

EXAFS spectra representing catalyst/support combinations, $Ir_4/\gamma\text{-}Al_2O_3$, $Ir_6/\gamma\text{-}Al_2O_3$, and Ir_4/MgO, show that the cluster frames were maintained before, during (Table 5), and after catalysis of propene hydrogenation, provided that the conditions were mild (*e.g.*, room temperature and 1 atm),[98,112] but when the temperature of catalysis reached about 423 K, the metals aggregated on the support. The data obtained at the lower temperatures are consistent with the inference that the supported clusters themselves are the catalytically active species.

In prospect, structurally well-defined supported metal clusters provide the opportunity for resolving support from cluster-size effects in catalysis.[113] A family of supported iridium clusters and particles was prepared from $Ir_4(CO)_{12}$ on $\gamma\text{-}Al_2O_3$.[114] The smallest clusters were approximately Ir_4, and samples with larger clusters and particles were prepared by treating $Ir_4/\gamma\text{-}Al_2O_3$ in H_2 under various conditions to cause aggregation and vary the average cluster or particle size. The catalytic activity for toluene hydrogenation was measured for each sample. The rate per exposed Ir atom increased by two orders of magnitude as the cluster/particle size increased, becoming independent of particle size when the average particle contained about 100 atoms.[114] The data characterizing the larger particles conform to the expected pattern for the "structure-insensitive" hydrogenation reaction, but those for the smaller clusters and particles do not. (A "structure-insensitive" reaction is one that takes place at approximately the same rate per exposed metal atom, independent of the face of the metal crystal that is exposed or the average size of the metal particle in the catalyst.[115]). The cluster size dependence of the catalytic activity is not yet explained.

One of the most thoroughly investigated examples of catalysis by supported metal clusters is hydrogenation of alkenes catalyzed by MgO- and $\gamma\text{-}Al_2O_3$-supported iridium (Ir_4 and Ir_6), with characterization of the catalysts in the working state by IR and EXAFS spectroscopies.[116,117] Similar data were reported for MgO-supported Rh_6.[118] The data show that the supports act as ligands; thus, Ir_4 on MgO was found to be an order of magnitude more active than Ir_4 on $\gamma\text{-}Al_2O_3$. The data characterize the structures of working catalysts, including the Ir_4 and Ir_6 cluster frames (which remained intact during reaction), the cluster–support interface, and the ligands formed during alkene hydrogenation. On Ir_4, for example, propene forms both unreactive (inhibitor) ligands (propylidyne) and catalytic intermediates, identified by IR spectroscopy as propyl and π-bonded propene; the support affects which of these hydrocarbon ligands predominate. The reaction intermediates influence the Ir–Ir distance in the clusters and the distance between the Ir atoms and the oxygen atoms of the support that are the longer (non-bonding) distances. Changes in the Ir–Ir and Ir–support oxygen distances ensued when the reactants were brought in contact with the catalyst, as shown schematically in Fig. 13. The data indicate that the reaction intermediates and the support are mutually interactive ligands.[116]

The Ir_4 clusters supported on $\gamma\text{-}Al_2O_3$ provide an example to contrast the reactivity of supported metal clusters with that of extended metal surfaces, such as those in the supported particles of metal in typical supported metal catalysts. The comparison is based on observations of the reactions of propene and hydrogen with the supported clusters (Fig. 14).[98] Propylidyne was formed from propene on Ir_4 at 298 K; it did not undergo isotopic exchange in the presence of D_2 at 298 K and was found to be stable in He or H_2 as the sample was heated to 523 K. In contrast, propylidyne chemisorbed on extended metal surfaces is hydrogenated to give propane in the presence of H_2 (or D_2) and exchanges hydrogen with gaseous D_2 at room temperature; in the absence of H_2, it decomposes thermally to give hydrocarbon fragments at temperatures much less than 523 K. Decomposition of propylidyne on the Ir_4 clusters did not take place until the temperature was raised beyond about 523 K, and the products formed on the supported clusters were markedly different from those observed for the reaction on the extended metal surface, with the reaction on the clusters evidently involving the support (Fig. 14). The difference in reactivities of propylidyne on clusters and on extended metal

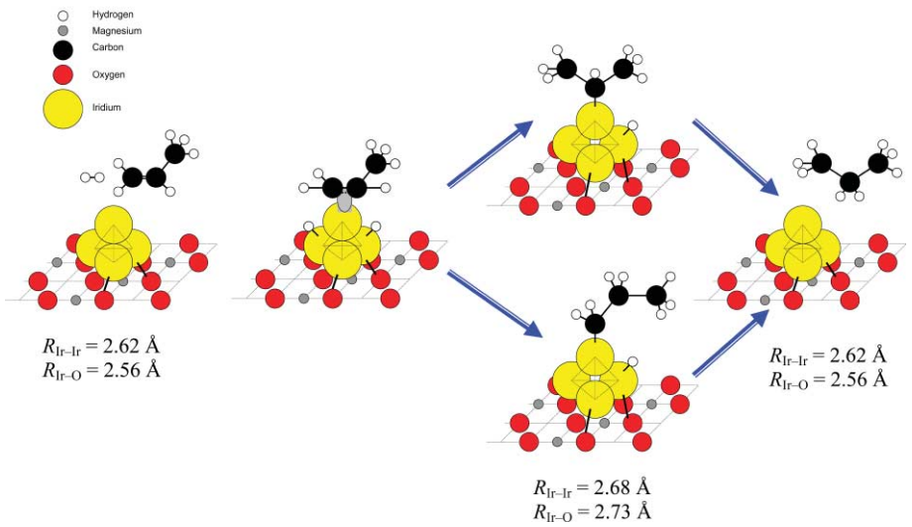

Fig. 13 Schematic representation of the hydrogenation of propene on MgO-supported Ir_4. Propene is initially π-bonded to the cluster then hydrogenated to give 1-propyl or 2-propyl, which is hydrogenated to give propane. The Ir–Ir and longer (non-bonding) Ir–O distances change as shown.[116]

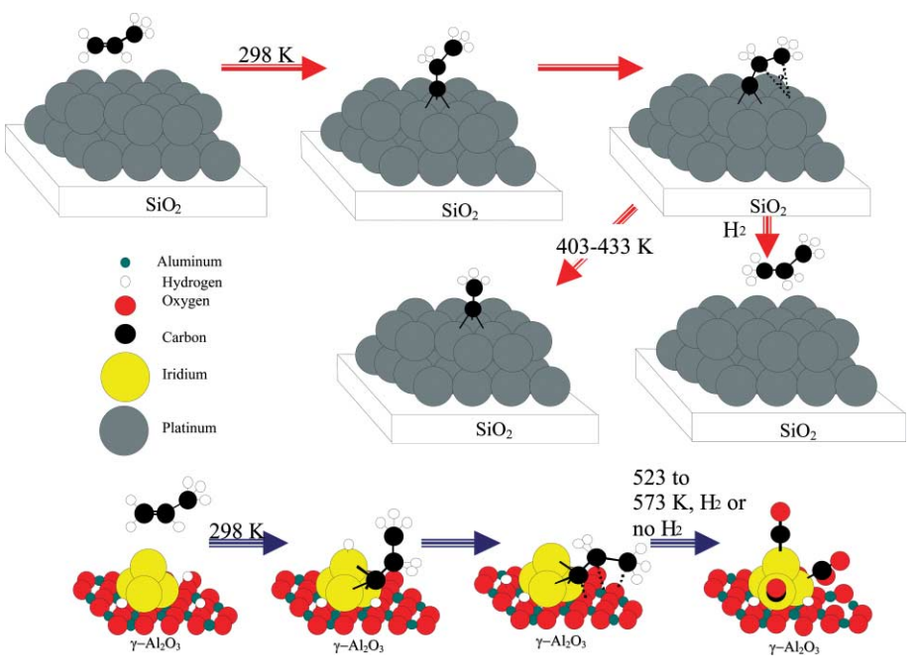

Fig. 14 Schematic representation of the stability and reactivity of propene on $Ir_4/\gamma\text{-}Al_2O_3$ and on extended metal surfaces (illustrated by particles of platinum supported on SiO_2).[98]

surfaces implies that ensembles of metal atoms larger than those offered by the clusters are needed for the reactions that occur readily on the extended metal surface. This geometric effect complements the ligand effects referred to in the preceding paragraph. Taken together, these effects indicate opportunities for discovering new chemistry with small supported metal clusters.

Supported gold cluster catalysts have drawn wide attention recently because, in contrast to extended surfaces of gold, they have high catalytic activities for CO oxidation and other reactions.[119,120] We prepared supported gold clusters of various average sizes on MgO by gentle sintering of the metal originally present in the supported mononuclear gold complex mentioned above $(Au^{III}(CH_3)_2\{OMg\}_2)$.[62] IR and EXAFS spectra were collected during ethene hydrogenation catalysis at steady state. The results shown in Fig. 15 indicate that the most active catalyst was the supported mononuclear gold complex, and there is no evidence that the clusters themselves are catalytically active for alkene hydrogenation, as the catalysts containing gold clusters also contained cationic gold (evidently mononuclear

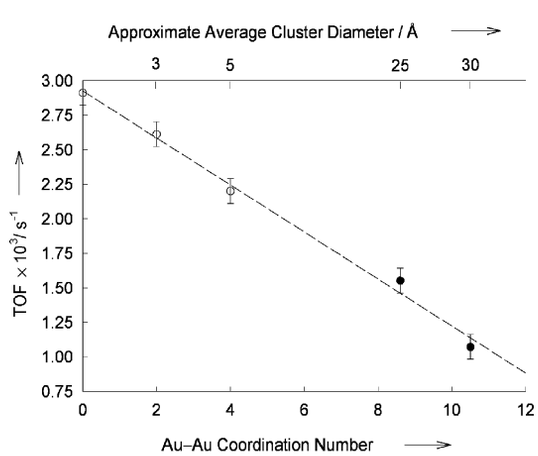

Fig. 15 Activities (turnover frequencies, TOF) of MgO-supported catalysts containing cationic gold and (except in the most active catalyst) gold clusters for ethene hydrogenation at 760 Torr and 353 K (ethene partial pressure, P_{ethene}, 40 Torr; $P_{hydrogen}$, 160 Torr; the balance He). Note the non-linearity of the scale at the top.[62]

gold complexes), as indicated by XANES data giving evidence of Au(III).

The supported clusters described in this account have strong connections to industrial supported metal catalysts, although the clusters or particles in industrial catalysts are much less uniform and less susceptible to incisive structural characterization than those considered here. Some industrial catalysts incorporate metal clusters of only a few metal atoms each, for example, platinum clusters in zeolite LTL for alkane dehydrocyclization.[121–123] EXAFS and transmission electron microscopy indicate that the clusters contain about 5–12 atoms each, on average, in well-prepared catalysts formed from tetraammineplatinum nitrate.[121–123] PdPt clusters of approximately this size are inferred to be present in zeolite-supported catalysts for aromatic hydroprocessing in the presence of sulfur to meet stringent fuel quality specifications; such small clusters are resistant to poisoning by sulfur.[124,125] Furthermore, two- and three-atom clusters of platinum on γ-Al_2O_3 (Pt/γ-Al_2O_3) were observed by scanning transmission electron microscopy, along with larger clusters, in γ-Al_2O_3-supported platinum catalysts prepared from a platinum ammine salt.[126]

Results characterizing structurally simple supported metal clusters are expected to continue to provide fundamental understanding that pertains to industrial supported metal catalysts.

Acknowledgements

This work was supported by the U.S. Department of Energy, Office of Energy Research, Office of Basic Energy Sciences, contract FG02-87ER13790, and a gift from Ford Motor Co.

References

1 F. Helfferich, *Ionenaustaucher. Band I. Grundlagen*, Verlag Chemie, Berlin, 1959.
2 I. R. Baxendale, S. V. Ley and C. Piutti, *Angew. Chem., Int. Ed.*, 2002, **41**, 2194.
3 (*a*) P. M. Maitlis, A. Haynes, G. J. Sunley and M. J. Howard, *J. Chem. Soc., Dalton Trans.*, 1996, **11**, 2187; (*b*) N. Yoneda, S. Kusane, M. Yasui, P. Pujado and S. Wilcher, *Appl. Catal. A*, 2001, **221**, 253.
4 D. E. De Vos, M. Dams, B. F. Sels and P. A. Jacobs, *Chem. Rev.*, 2002, **102**, 3640.
5 B. C. Gates, *J. Mol. Catal. A*, 2000, **163**, 55.
6 B. C. Gates, in *Catalysis by Di- and Polynuclear Metal Cluster Complexes*, eds. R. D. Adams and F. A. Cotton, Wiley–VCH, Weinheim, 1998, p. 509.
7 B. C. Gates, *Top. Catal.*, 2001, **14**, 173.
8 *Studies in Surface Science and Catalysis*, eds. Y. I. Yermakov, B. N. Kuznetsov, and V. A. Zakharov, Elsevier, Amsterdam, 1981, vol. 8.
9 D. G. H. Ballard, *Adv. Catal.*, 1973, **23**, 263.
10 *Surface Organometallic Chemistry: Molecular Approaches to Surface Catalysis, NATO ASI series*, eds. J-M. Basset, B. C. Gates, J.-P. Candy, A. Choplin, M. Leconte, F. Quignard, and C. Santini, Kluwer, Dordrecht, 1988, Vol. 231.
11 J. F. Walzer, Jr., *US Pat*., 5643847, 1997.
12 1996, vol. 1; *Applied Homogeneous Catalysis with Organometallic Compounds*, eds. B. Cornils and W. A. Herrmann, VCH, Weinheim, 2nd edn., 2002.
13 F. R. Hartley, in *Supported Metal Complexes: A new Generation of Catalysts*, Reidel, Boston, MA, 1985.
14 (*a*) G. G. Hlatky, *Chem. Rev.*, 2000, **100**, 1347; (*b*) G. Fink, B. Steinmetz, J. Zechlin, C. Przybyla and B. Tesche, *Chem. Rev.*, 2000, **100**, 1377; (*c*) H. H. Brintzinger, D. Fischer, R. Mülhaupt, B. Rieger and R. M. Waymouth, *Angew. Chem., Int. Ed. Engl.*, 1995, **34**, 1143.
15 F. J. Karol, C. Wu, W. T. Reichle and N. J. Maraschin, *J. Catal.*, 1979, **60**, 68.
16 A. Andresen, H. G. Cordes, J. Herwig, W. Kaminsky, A. Merck, R. Mottweiler, J. Pein, J. Hansjoerg and H.-J Vollmer, *Angew. Chem., Int. Ed. Engl.*, 1976, **15**, 630.
17 V. Dufaud and J.-M. Basset, *Angew. Chem., Int. Ed.*, 1998, **37**, 806.
18 V. Vidal, A. Théolier, J. Thivolle-Cazat and J.-M. Basset, *Science*, 1997, **276**, 99.
19 H. H. Lamb, B. C. Gates and H. Knözinger, *Angew. Chem., Int. Ed. Engl.*, 1988, **27**, 1127.
20 J.-M. Basset, F. Lefebvre and C. Santini, *Coord. Chem. Rev.*, 1998, **178–180**, 1703.
21 P. Dufour, C. Houtman, C. C. Santini, C. Nédez, J.-M. Basset, L. Y. Hsu and S. G. Shore, *J. Am. Chem. Soc.*, 1992, **114**, 4248.
22 H. C. Foley, S. J. DeCanio, K. D. Tau, K. J. Chao, J. H. Onuferko, C. Dybowski and B. C. Gates, *J. Am. Chem. Soc.*, 1983, **105**, 3074.
23 P. Dufour, C. Houtman, C. C. Santini and J.-M. Basset, *J. Mol. Catal.*, 1992, **77**, 257.
24 A. Brenner, in *Metal Clusters*, ed. M. Moskovits, Wiley, New York, 1986.
25 P. S. Kirlin, H. Knözinger and B. C. Gates, *J. Phys. Chem.*, 1990, **94**, 8451.
26 O. Alexeev and B. C. Gates, *Top. Catal.*, 2000, **10**, 273.
27 (*a*) F. J. Feher, T. A. Budzichowski and K. J. Weller, *J. Am. Chem. Soc.*, 1989, **111**, 7288; (*b*) F. J. Feher, D. A. Newman and J. F. Walzer, *J. Am. Chem. Soc.*, 1989, **111**, 1741; (*c*) F. J. Feher and K. J. Weller, *Organometallics*, 1990, **9**, 2638; (*d*) F. J. Feher and D. A. Newman, *J. Am. Chem. Soc.*, 1990, **112**, 1931; (*e*) J. R. Severn, R. Duchateau, R. A. van Santen, D. D. Ellis and A. L. Spek, *Organometallics*, 2002, **21**, 4; (*f*) T. W. Dijkstra, R. Duchateau, R. A. van Santen, A. Meetsma and G. P. A. Yap, *J. Am. Chem. Soc.*, 2002, **124**, 9856; (*g*) R. Duchateau, *Chem. Rev.*, 2002, **102**, 3525.
28 F. J. Feher, J. J. Schwab, S. H. Phillips, A. Eklund and E. Martinez, *Organometallics*, 1995, **14**, 4452.
29 F. J. Feher and T. A. Budzichowski, *Polyhedron*, 1995, **14**, 3239.
30 (*a*) W. A. Weber and B. C. Gates, *J. Phys. Chem. B*, 1997, **101**, 10423; (*b*) W. A. Weber and B. C. Gates, *J. Catal.*, 1998, **180**, 207; (*c*) L. Basini, R. Patrini, A. Aragno and B. C. Gates, *J. Mol. Catal.*, 1991, **70**, 29.
31 J. F. Goellner, B. C. Gates, G. N. Vayssilov and N. Rösch, *J. Am. Chem. Soc.*, 2000, **122**, 8056.
32 H. Miessner, I. Burkhardt, D. Gutschick, A. Zecchina, C. Morterra and G. Spoto, *J. Chem. Soc., Faraday Trans. 1*, 1989, **85**, 2113.
33 C. J. Papile and B. C. Gates, *Langmuir*, 1992, **8**, 74.
34 P. S. Kirlin, F. A. DeThomas, J. W. Bailey, H. S. Gold, C. Dybowski and B. C. Gates, *J. Phys. Chem.*, 1986, **90**, 4882.
35 N. D. Triantafillou, S. K. Purnell, C. J. Papile, J.-R. Chang and B. C. Gates, *Langmuir*, 1994, **10**, 4077.
36 P. S. Kirlin, F. B. M. van Zon, D. C. Koningsberger and B. C. Gates, *J. Phys. Chem.*, 1990, **94**, 8439.
37 J.-R. Chang, L. U. Gron, A. Honji, K. M. Sanchez and B. C. Gates, *J. Phys. Chem.*, 1991, **95**, 9944.
38 A. Honji, L. U. Gron, J.-R. Chang and B. C. Gates, *Langmuir*, 1992, **8**, 2715.
39 (*a*) S. K. Purnell, X. Xu, D. W. Goodman and B. C. Gates, *Langmuir*, 1994, **10**, 3057; (*b*) S. K. Purnell, X. Xu, D. W. Goodman and B. C. Gates, *J. Phys. Chem.*, 1994, **98**, 4076.
40 A. Hu, K. M. Neyman, M. Staufer, T. Belling, B. C. Gates and N. Rösch, *J. Am. Chem. Soc.*, 1999, **121**, 4522.
41 P. S. Kirlin, F. A. DeThomas, J. W. Bailey, K. Moller, H. S. Gold, C. Dybowski and B. C. Gates, *Surface Sci.*, 1986, **175**, L707.
42 B. Enderle and B. C. Gates, *Phys. Chem. Chem. Phys.*, submitted.
43 F. B. M. Duivenvoorden, D. C. Koningsberger, Y. S. Uh and B. C. Gates, *J. Am. Chem. Soc.*, 1986, **108**, 6254.
44 K. Asakura, M. Yamada, Y. Iwasawa and H. Kuroda, *Chem. Lett.*, 1985, 511.
45 N. Binsted, J. Evans, G. N. Greaves and R. J. Price, *Organometallics*, 1989, **8**, 613.
46 S. E. Deutsch, J.-R. Chang and B. C. Gates, *Langmuir*, 1993, **9**, 1284.
47 V. Vidal, A. Théolier, J. Thivolle-Cazat, J.-M. Basset and J. Corker, *J. Am. Chem. Soc.*, 1996, **118**, 4595.
48 J. Corker, F. Lefebvre, C. Lécuyer, V. Dufaud, F. Quignard, A. Choplin, J. Evans and J.-M. Basset, *Science*, 1996, **271**, 966.
49 L. Lefort, M. Chabanas, O. Maury, D. Meunier, C. Copéret, J. Thivolle-Cazat and J.-M. Basset, *J. Organomet. Chem.*, 2000, **593–594**, 96.
50 G. Saggio, A. de Mallmann, B. Maunders, M. Taoufik, J. Thivolle-Cazat and J.-M. Basset, *Organometallics*, 2002, **21**, 5167.
51 H. Miessner, *J. Am. Chem. Soc.*, 1994, **116**, 11522.
52 E. A. Wovchko and J. T. Yates, Jr., *Langmuir*, 1999, **15**, 3506.
53 C. Copéret, M. Chabanas, R. P. Saint-Arroman and J.-M. Basset, *Angew. Chem., Int. Ed.*, 2003, **42**, 156.
54 S. L. Scott, P. Dufour, C. C. Santini and J.-M. Basset, *J. Chem. Soc., Chem. Commun.*, 1994, 2011.
55 J. Guzman and B. C. Gates, *J. Phys. Chem. B*, 2003, **107**, 2242.
56 J. Guzman and B. C. Gates, *J. Phys. Chem. B*, 2002, **106**, 7659.
57 F. S. Lai and B. C. Gates, to be published.
58 O. Maury, L. Lefort, V. Vidal, J. Thivolle-Cazat and J.-M. Basset, *Angew. Chem., Int. Ed.*, 1999, **38**, 1952.

59 C. Copéret, O. Maury, J. Thivolle-Cazat and J.-M. Basset, *Angew. Chem., Int. Ed.*, 2001, **40**, 2331.
60 M. Chabanas, V. Vidal, C. Copéret, J. Thivolle-Cazat and J.-M. Basset, *Angew. Chem., Int. Ed.*, 2002, **39**, 1962.
61 P. Cossee, *J. Catal.*, 1964, **3**, 80.
62 J. Guzman and B. C. Gates, *Angew. Chem., Int. Ed.*, 2003, **42**, 690.
63 B. C. Gates, *Chem. Rev.*, 1995, **95**, 511.
64 S. Kawi and B. C. Gates, *Inorg. Chem.*, 1992, **31**, 2939.
65 S. Kawi, Z. Xu and B. C. Gates, *Inorg. Chem.*, 1994, **33**, 503.
66 (*a*) H. H. Lamb, T. R. Krause and B. C. Gates, *J. Chem. Soc., Chem. Commun.*, 1986, **11**, 821; (*b*) H. H. Lamb, A. S. Fung, P. A. Tooley, J. Puga, T. R. Krause, M. J. Kelley and B. C. Gates, *J. Am. Chem. Soc.*, 1989, **111**, 8367; (*c*) E. Cariati, D. Roberto, Dominique and R. Ugo, *J. Cluster Sci.*, 1998, **9**, 329; (*d*) E. Cariati, P. Recanati, D. Roberto and R. Ugo, *Organometallics*, 1998, **17**, 1266.
67 E. Cariati, E. Lucenti, D. Roberto and R. Ugo, *Spec. Publ.-R. Soc. Chem.*, 1998, **216**, 214.
68 G. Panjabi, S. N. Salvi, B. A. Phillips, V. I. Bhirud and B. C. Gates, to be published.
69 L. F. Allard, G. A. Panjabi, S. N. Salvi and B. C. Gates, *Nano Lett.*, 2002, **2**, 381.
70 J.-M. Basset and R. Ugo, *Aspects Homogeneous Catal.*, 1977, **3**, 137.
71 O. S. Alexeev, D.-W. Kim and B. C. Gates, *J. Mol. Catal. A*, 2000, **162**, 67.
72 A. K. Smith, A. Theolier, J.-M. Basset, R. Ugo, D. Commereuc and Y. Chauvin, *J. Am. Chem. Soc.*, 1978, **100**, 2590.
73 O. Alexeev and B. C. Gates, *J. Catal.*, 1998, **176**, 310.
74 T. Beutel, S. Kawi, S. K. Purnell, H. Knözinger and B. C. Gates, *J. Phys. Chem.*, 1993, **97**, 7284.
75 L. Malatesta, G. Caglio and M. Angoletta, *Inorg. Synth.*, 1972, **13**, 95.
76 G. C. Bruce and S. R. Stobart, *Inorg. Chem.*, 1988, **27**, 3879.
77 A. Mezzetti, E. Zangrando, A. Del Zotto and P. Rigo, *J. Chem. Soc., Chem. Commun.*, 1994, 1597.
78 F. Dawans, J. Dewailly, J. Meunier-Piret and P. Piret, *J. Organomet. Chem.*, 1974, **76**, 53.
79 C. J. Besecker, W. G. Klemperer and V. W. Day, *J. Am. Chem. Soc.*, 1982, **104**, 6158.
80 V. G. Albano, G. Ciani and M. Manassero, *J. Organomet. Chem.*, 1970, **25**, C55.
81 R. R. Schrock, J. S. Murdzek, J. H. Freudenberger, M. R. Churchill and J. W. Ziller, *Organometallics*, 1986, **5**, 25.
82 H. I. Hyden, H. G. Alt and R. D. Rogers, *J. Organomet. Chem.*, 1987, **323**, 339.
83 V. W. Day, W. G. Klemperer and D. J. Main, *Inorg. Chem.*, 1990, **29**, 2345.
84 C. J. Besecker, V. W. Day and W. G. Klemperer, *Organometallics*, 1985, **4**, 564.
85 B. Nuber, F. Oberdorfer and M. L. Ziegler, *Acta Crystallogr., Sect. B*, 1981, **37**, 2062.
86 G. Ciani, A. Sironi and A. Abinati, *Gazz. Chim. Ital.*, 1979, **109**, 615.
87 T. Beringhelli, G. Ciani, G. D'Alfonso, A. Sironi and M. Freni, *J. Chem. Soc., Dalton Trans.*, 1985, 1507.
88 V. W. Day, W. G. Klemperer, S. P. Lockledge and D. J. Main, *J. Am. Chem. Soc.*, 1990, **112**, 2031.
89 A. M. Ferrari, K. M. Neyman, M. Mayer, M. Staufer, B. C. Gates and N. Rösch, *J. Phys. Chem. B*, 1999, **103**, 5311.
90 J. F. Goellner, K. M. Neyman, M. Mayer, F. Nörtemann, B. C. Gates and N. Rösch, *Langmuir*, 2000, **6**, 2736.
91 D. C. Koningsberger and B. C. Gates, *Catal. Lett.*, 1992, **14**, 271.
92 G. N. Vayssilov, B. C. Gates and N. Rösch, *Angew. Chem., Int. Ed.*, 2003, **42**, 1391.
93 G. N. Vayssilov and N. Rösch, *J. Am. Chem. Soc.*, 2002, **124**, 3783.
94 A. S. Fung, P. A. Tooley, M. J. Kelly, D. C. Koningsberger and B. C. Gates, *J. Phys. Chem.*, 1991, **95**, 225.
95 F. A. Cotton, C. Lin and C. A. Murillo, *Acc. Chem. Res.*, 2001, **34**, 759.
96 W. C. Conner, Jr. and J. L. Falconer, *Chem. Rev.*, 1995, **95**, 759.
97 V. I. Bhirud, J. F. Goellner, A. M. Argo and B. C. Gates, to be published.
98 A. M. Argo, J. F. Goellner, B. L. Phillips, G. A. Panjabi and B. C. Gates, *J. Am. Chem. Soc.*, 2001, **123**, 2275.
99 S. N. Reifsnyder, M. M. Otten and H. H. Lamb, *Catal. Today*, 1998, **39**, 317.
100 G. Schulz-Ekloff and S. Ernst, *Prep. Solid Catal.*, 1999, 405.
101 (*a*) N. Jaeger, P. Plath and G. Schulz-Ekloff, *Acta Phys. Chem.*, 1985, **31**, 189; (*b*) A. Tonscheidt, P. L. Ryder, N. I. Jaeger and G. Schulz-Ekloff, *Zeolites*, 1996, **16**, 271.
102 H. F. J. Van't Blik, J. B. A. D. van Zon, T. Huizinga, J. C. Vis, D. C. Koningsberger and R. Prins, *J. Am. Chem. Soc.*, 1985, **107**, 3139.
103 P. Braunstein and J. Rosé, in *Metal Clusters in Chemistry*, eds. P. Braunstein, L. A. Oro and P. R. Raithby, Wiley–VCH, Weinheim, 1999, p. 616.
104 O. S. Alexeev and B. C. Gates, *Ind. Eng. Chem. Res.*, 2003, **42**, 1571.
105 O. S. Alexeev, G. W. Graham, M. Shelef, R. D. Adams and B. C. Gates, *J. Phys. Chem. B*, 2002, **106**, 4697.
106 S. Kawi, O. Alexeev, M. Shelef and B. C. Gates, *J. Phys. Chem.*, 1995, **99**, 6926.
107 O. Alexeev, S. Kawi, M. Shelef and B. C. Gates, *J. Phys. Chem.*, 1996, **100**, 253.
108 A. S. Fung, M. J. Kelley, D. C. Koningsberger and B. C. Gates, *J. Am. Chem. Soc.*, 1997, **119**, 5877.
109 O. Alexeev, M. Shelef and B. C. Gates, *J. Catal.*, 1996, **164**, 1.
110 O. Alexeev, G. W. Graham, M. Shelef and B. C. Gates, *J. Catal.*, 2000, **190**, 157.
111 D. S. Shephard, T. Maschmeyer, G. Sankar, J. M. Thomas, D. Ozkaya, B. F. G. Johnson, R. Raja, R. D. Oldroyd and R. G. Bell, *Chem. Eur. J.*, 1998, **4**, 1214.
112 G. Panjabi, A. M. Argo and B. C. Gates, *Chem. Eur. J.*, 1999, **5**, 2417.
113 Z. Xu, F.-S. Xiao, S. K. Purnell, O. Alexeev, S. Kawi, S. E. Deutsch and B. C. Gates, *Nature (London)*, 1994, **372**, 346.
114 F.-S. Xiao, W. A. Weber, O. Alexeev and B. C. Gates, in *Proceedings of the Eleventh International Congress on Catalysis (Stud. Surf. Sci. Catal. B)*, 1996, vol. 101, p. 1135.
115 M. Boudart and G. Djéga-Mariadassou, *Kinetics of Heterogeneous Catalytic Reactions*, Princeton University Press, Princeton, NJ, 1984.
116 A. M. Argo, J. F. Odzak, F. S. Lai and B. C. Gates, *Nature (London)*, 2002, **415**, 623.
117 A. M. Argo, J. F. Odzak and B. C. Gates, *J. Am. Chem. Soc.*, 2003, **125**, 7107.
118 A. M. Argo and B. C. Gates, *J. Phys. Chem. B*, 2003, **107**, 5519.
119 (*a*) M. Haruta, *Catal. Today*, 1997, **36**, 153; (*b*) M. Haruta and M. Daté, *Appl. Catal. A*, 2001, **222**, 427.
120 G. J. Hutchings, *Catal. Today*, 2002, **72**, 11.
121 R. E. Jentoft, M. Tsapatsis, M. E. Davis and B. C. Gates, *J. Catal.*, 1998, **179**, 565.
122 M. Vaarkamp, F. S. Modica, J. T. Miller and D. C. Koningsberger, *J. Catal.*, 1993, **144**, 611.
123 (*a*) J. T. Miller, B. L. Meyers, F. S. Modica, G. S. Lane, M. Vaarkamp and D. C. Koningsberger, *J. Catal.*, 1993, **143**, 395; (*b*) J. T. Miller, N. G. B. Agrawal, G. S. Lane and F. S. Modica, *J. Catal.*, 1996, **163**, 106.
124 (*a*) H. Yasuda, T. Kameoka, T. Sato, N. Kijima and Y. Yoshimura, *Appl. Catal. A*, 1999, **185**, L199; (*b*) H. Yasuda, T. Sato and Y. Yoshimura, *Catal. Today*, 1999, **50**, 63.
125 W. C. Baird, G. B. McVicker, Jr., J. J. Schorfheide, D. P. Klein, S. Hantzer, M. Daage, M. S. Touvelle, E. S. Ellis, D. E. W. Vaughan and J. G. Chen, *US Pat.*, 5935420, 1997.
126 P. D. Nellist and S. J. Pennycook, *Science*, 1996, **274**, 413.